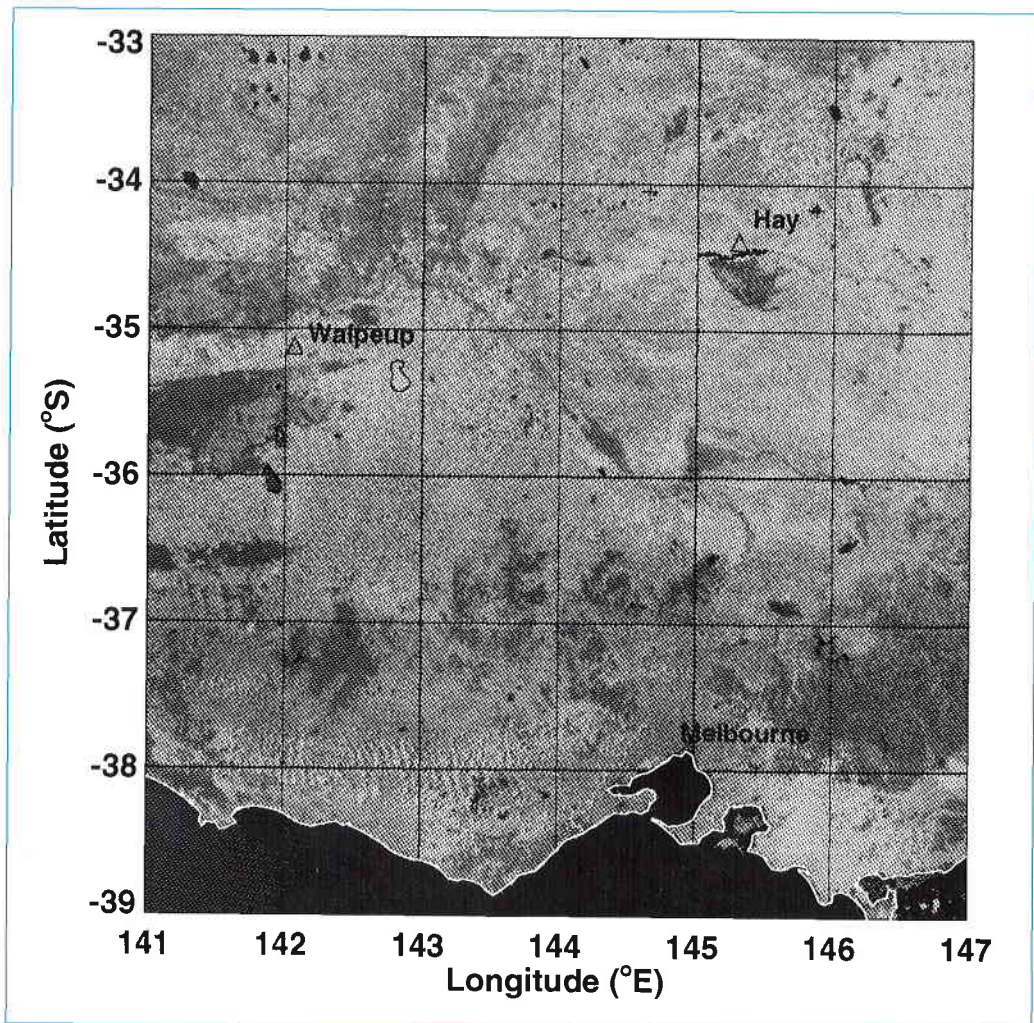




Validation Data for Land Surface Temperature Determination from Satellites

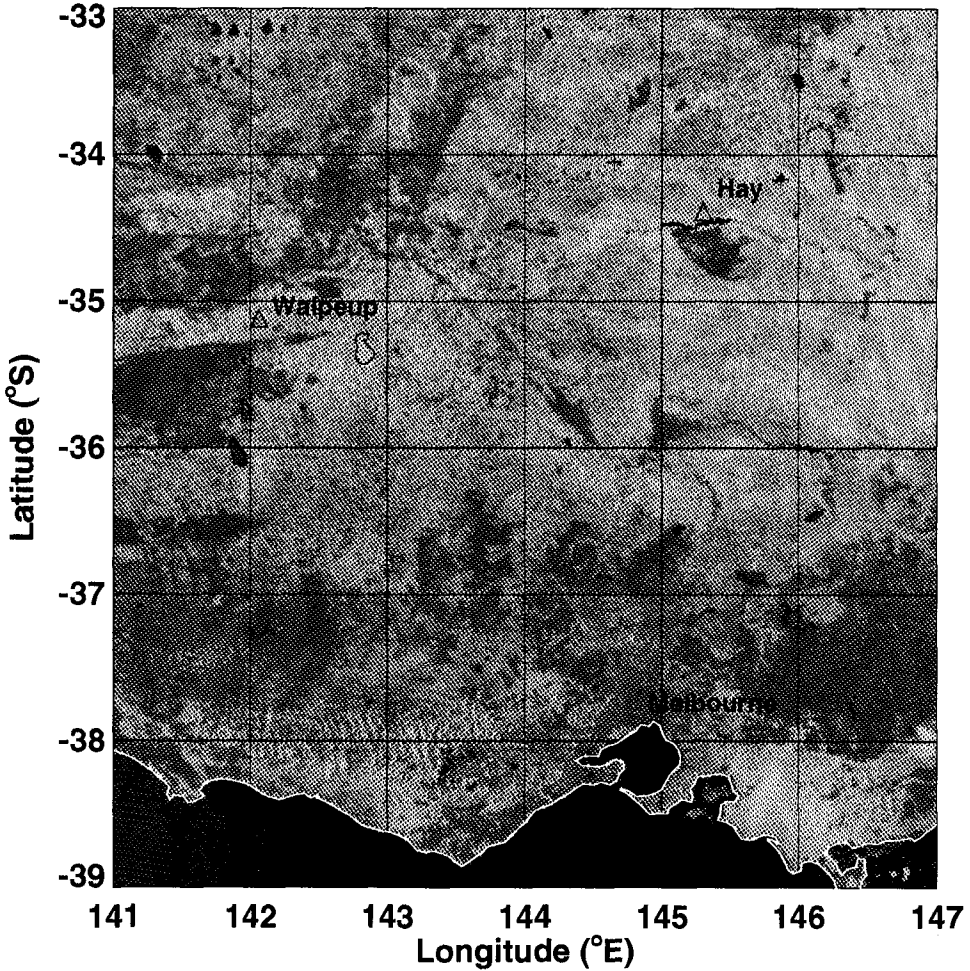
A. J. Prata





Validation Data for Land Surface Temperature Determination from Satellites

A. J. Prata



National Library of Australia Cataloguing-in-Publication Entry

Prata, A. J.

Validation data for land surface temperature determination from satellites.

Bibliography.

ISBN 0 643 05600 9.

1. Earth temperature- Remote sensing. 2. Earth temperature- Measurement.
3. Earth temperature- Australia- Measurement. 4. Artificial satellites in earth sciences.
I. CSIRO, Division of Atmospheric Research. II Title. (Series: Division of Atmospheric
Research Technical Paper No. 33)

551.14

CSIRO, Division of Atmospheric Research Technical Papers may be issued out of sequence.

Front cover: AVHRR channel 2 image of Victoria and southern New South Wales, Australia showing the locations of the field sites used to obtain land surface temperature validation data.

© CSIRO Australia 1994

Printed on recycled and environmentally friendly paper

Validation Data for Land Surface Temperature Determination from Satellites

A. J. Prata

CSIRO, Division of Atmospheric Research,
Private Bag 1, Mordialloc, VIC 3195, Australia

Abstract

There has been a paucity of appropriate ground-truth data for validating satellite estimates of land surface temperatures, due mostly to the difficulties associated with obtaining representative surface temperatures over an area comparable in size to that from a satellite measurement (typically about 1 km² in area). For the express purpose of obtaining ground-truth data, field experiments were set up in two semi-arid regions of Australia. The data from these field experiments are reported here in the form of tables. The tables contain ground-truth surface temperatures, satellite brightness temperatures, and the relevant satellite and solar geometries. A description of the sites, the measurement techniques and accuracies, and some climatological variables are also provided.

1. Introduction

For the last few years a field experiment has been conducted to validate satellite derived land surface temperatures (LSTs). This work has involved devising novel field equipment to obtain representative spatial information for comparison with satellite radiometer data. New LST algorithms have been formulated and a system - CSIRO Intelligent Data Acquisition and Telemetry network (CSIDAT) has been developed for measuring in situ temperatures over large areas (up to 15x15 km²).

Routine land surface temperature measurements from satellites are not available because of difficulties in determining atmospheric effects and surface effects (e.g. emissivities) which cause perturbations to the infrared measurements.

Techniques for deriving LSTs from the Advanced Very High Resolution Radiometer (AVHRR) (e.g. the split-window method) are applicable over the land if the surface emissivity and its spectral dependence in the infrared window are both known (Prata, 1993). To determine the accuracy of the satellite LST estimates they must be validated against in situ or ground-based remotely sensed measurements. Meteorological stations routinely make air temperature measurements at about 1.5 m above the surface. These data cannot be used to validate the radiometric surface temperature that a satellite infrared radiometer measures because often there are very large temperature gradients between the surface and the first few metres of the atmospheric boundary layer.

In the past, the *in situ* measurements have been made using ground-based wide-band (8-14 μm) radiometers. The radiometer is typically mounted a few metres above the surface and measures an area of the surface a few metres in diameter. For most natural surfaces, the scale of temperature and emissivity variability is from a few centimetres up to many kilometres and so the ground based radiometric measurement may be quite unrepresentative of the satellite measurements.

An alternative approach is to use contact thermometers which measure the thermodynamic temperature rather than the radiometric temperature. This measurement, although closer to the "true" surface temperature is difficult to make because good contact is very hard to achieve in practice. The approach taken here is to place a sufficient number of contact solid state temperature transducers over a large area ($\approx 1 \text{ km}^2$), and use the average temperatures to compare with the satellite measurements. A description of the method used to obtain the validation data and tabulations are provided in this report.

Climatological values of the relevant atmospheric parameters and some limited emissivity measurements are provided for the sites to allow users of the validation data to test and develop models for LST estimation.

2. Experimental procedures

Over the land, temperature variability is high (several degrees Celsius per metre or more may be typical), and it is necessary to make temperature measurements at several locations within the field-of-view of the satellite radiometer to make meaningful comparisons. With this in mind, a system has been devised that can be deployed over a large area and can operate automatically with little maintenance. The basic equipment consists of a central site with a capability of accepting up to 32 channels of data, an ARGOS transmitter and a back-up data store. The site is self-contained and powered by batteries that are recharged using solar panels. Eight "satellite stations" are connected to the central site via underground cables. Each satellite station is instrumented and collects data which are relayed back to the central site. The satellite stations can be many kilometres from the central site:- the distance being limited by the practicality of the underground cabling*. At the central site the data are collected, compressed and put into a form suitable for transmission to the ARGOS system on board the NOAA satellites. This strategy ensures that the *in situ* data are simultaneous with the AVHRR measurements. With two satellites operational, a system deployed at a mid-latitude location can relay about 12 kbits of data per day. The data are received locally via a satellite reception facility and are available for analysis usually within 30 minutes of the overpass.

Because of its great flexibility, CSIDAT can be used in a variety of situations for monitoring several surface variables simultaneously. For example, measurements are being made of surface and air temperature, incoming solar radiation, reflected solar radiation, downwelling longwave radiation and wind speed at the same large site to infer the net surface radiation. A cellular telephone and modem can also be added, and optionally used as an alternative to using the ARGOS satellite system. The equipment described here has been deployed at two remote locations in Australia. These sites are briefly described in the following two subsections.

* An improved system, using radio frequency communication rather than underground cabling has recently been devised (see Prata et al., 1992).

2.1 The Walpeup site

The site is located in NW Victoria ($35^{\circ}11'58''\text{S}$, $142^{\circ}03'51''\text{E}$) in a wheat growing area. The climate is quite dry and the region is described as semi-arid (see Table 1).

The paddock chosen for deployment of the field instruments is on flat terrain of uniform surface composition, and consequently the spatial temperature variability is very low. Figure 1 (front cover) shows an AVHRR image of the region. Eight satellite stations and a central site were deployed measuring surface and air temperatures. Underground cabling was used at this site. Over the years the field has been ploughed bare, sown to wheat, then to barley and also has lain fallow. Measurements were made during the period March 1990 to July 1992. Figure 2 shows the central site within the large paddock when a mature crop of wheat was growing. Figure 3 depicts the configuration of the sensors at Walpeup. Further details concerning this site may be found in Prata et al. (1990).



Figure 2. Photograph of the central site within the wheat paddock at Walpeup, NW Victoria.

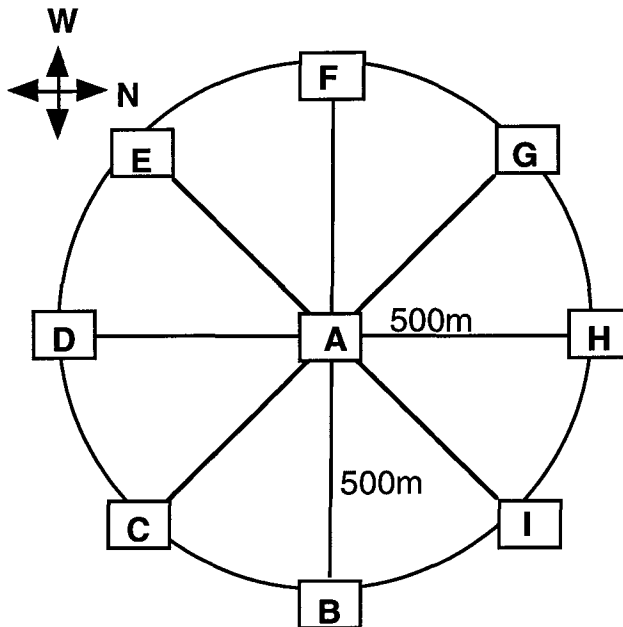


Figure 3. Sketch map showing the locations of the field instruments within the paddock at Walpeup, NW Victoria. The electronics boxes are numbered from A (central site) to I (NE site); each box controls two sensors. A total of 25 channels of data can be recorded: 18 channels measure temperatures at the surface or in the air; 7 channels record underground temperatures at the central site. The underground cabling is shown by the solid lines between the instrument boxes.

2.2 The Hay site

A CSIDAT system has also been deployed on the Uardry sheep station near the town of Hay in New South Wales, Australia. The climate of the region is very similar to that at Walpeup. Rainfall occurs mostly during the winter months, while the summers are hot and dry (see Table 1). The Murrumbidgee river flows east-west across the region about 10 km south of the field site. Like the Walpeup site, the spatial temperature variability is low.

This uniform site was selected by looking at clear nighttime AVHRR images of the area. A preliminary site was selected, and then a field trip undertaken to make a further assessment of the suitability of the site. The final locations of the instruments were made on the basis of ground cover, access and distance from obstructions. The instruments were deployed in the configuration of a cross with maximum length of 1 km, and RF communication was used. Table 2 shows the instruments used and their location.

At this site measurements are being made to infer the net radiation at the surface. An up-

ward looking pyranometer measures the downcoming solar flux, while three downward looking pyranometers measure the reflected flux. An upward looking pyrgeometer measures the downwelling longwave flux. Temperature transducers measure the ground temperature and air temperature at 1.0 m and two anemometers measure the wind speed at 3.0 m. The radiation instruments are mounted at the top of a mast 4 m high or at the end of a long boom about 3 m from the ground. These radiation measurements will not be reported here.

Data samples from the system are obtained at a rate compatible with ARGOS transmissions (i.e. every 200 s) and are logged to a data-logger every 5 minutes. During the satellite overpass, 256 bits of information are transmitted to the satellite every 200 s. The samples are tagged by site number and time stamped. All 9 stations are sampled within the 200 s time window. Because samples are logged every 5 min, it is possible to use these data to validate the Along Track Scanning Radiometer (ATSR) measurements (see section 4.3).

2.3 Temperature transducers

The devices used for measuring in situ temperatures are AD592 solid state temperature transducers. The AD592 is a two terminal monolithic integrated circuit temperature transducer that provides an output current proportional to absolute temperature. The range of applicability of the device is -25° to $+105^{\circ}\text{C}$. Once calibrated and trimmed, the AD592 is capable of a temperature measurement accuracy of 0.1°C , has a nonlinearity error of 0.1°C and a repeatability of 0.1°C per month. The typical response time of the device mounted on the surface of sand is 10-20 s. However, after potting and mounting, the measured response time is in the range 30-60 s. Photographs of the sensors mounted on the ground at Hay may be seen in Figure 8.

For use in the field, the sensors are mounted in plastic sleeves and potted in solastic cement to prevent water from reaching the electrical connections. The sensing surface area measures approximately 25 mm^2 , and the devices are secured to the surface by thin metal wires to avoid movement. No attempt has been made to ensure that the sensing surface (coloured black) has the same shortwave albedo and longwave emissivity as the surface being measured. Differences in albedo have been investigated by covering the sensor with highly reflective aluminium foil. Results from these experiments demonstrate that large differences (up to a few $^{\circ}\text{C}$) can occur during the day when the sun is shining, but negligible differences are observed at night. These experiments are reported in Prata (1994b).

3. Satellite data

The satellite data used in this study are derived from the AVHRRs on board the NOAA polar orbiting satellites and from the ATSR on board the polar orbiting ERS-1 satellite. Table 3 lists some of the characteristics of the AVHRR and ATSR relevant to this work.

AVHRR data are received locally in Melbourne and are processed using standard techniques (e.g. Planet, 1988). Nonlinearity corrections have been applied to channels 4 and 5 according to the look-up tables supplied by NOAA-NESDIS. A new scheme based on coefficients supplied by Dr Otis Brown (private communication) has recently been implemented. For the temperatures encountered at the field sites, the new scheme differs little from the NESDIS scheme. For consistency, all of the validation data presented in this report employed the new nonlinearity correction scheme.

Cloud detection was performed using thresholding for the infrared channels during the night

and for all channels, except channel 3, during the day. Additionally, statistics (mean and variance) of 3x3, 5x5 and 7x7 pixel blocks centred on the pixel closest to the field site were derived. These were used to check the spatial uniformity of the data. Data with a large channel 4 infrared variance ($>3.0^{\circ}\text{C}^2$ over 3x3 pixels) were immediately rejected. Nighttime data over land present the most difficult situation in which to detect cloudy pixels. For these cases, the in situ data have been used to assist in cloud detection. Whenever the in situ data are larger than the AVHRR channel 4 brightness temperatures by 8°C or more it is assumed that the pixel is cloudy. This test is based on the assumption that water vapour effects during the night are smaller than those during the day and from the fact that an analysis of cloud free daytime data shows that the in situ measurements never exceed the channel 4 brightness temperatures by more than 8°C . Nevertheless, it is not possible to be certain that some pixels in the nighttime data are not cloud contaminated. This highlights the need for improved nighttime cloud detection algorithms.

Accurate navigation of the data was achieved using ground control points (gcps). A general purpose satellite navigation software package was first used to locate the pixels on the earth's surface, and then gcps were used to adjust the image data linearly in latitude and/or longitude. This process was performed manually on each image to ensure an accurate navigation (subjectively). The largest discrepancies were usually in the along track direction (latitude) amounting to 5-10 pixels. The gcps were selected close to the field site around lake boundaries or bends in prominent rivers. The image shown on the Front Cover includes some of the features used to obtain accurate image navigation. For the Walpeup site, three lake boundaries near to the site were digitised and used to check navigational accuracy. For the Uardry site, a portion of the Murrumbidgee river, just south of the site, and two prominent features (marked by plus signs on the image) on lakes to the NE and NW of the site were digitised. The final rms geolocation accuracy of the image pixels close to the field site was estimated to be better than 1 pixel.

4. Tabulations

AVHRR validation data for both sites are presented in the form of Tables. Each table consists of up to 10 columns. These are:

- the date, in the format Day/Month/Year
- the time, in Universal Time (UT) Hours:Minutes
- channel 3 AVHRR satellite brightness temperature T_3 , in $^{\circ}\text{C}$
- channel 4 AVHRR satellite brightness temperature T_4 , in $^{\circ}\text{C}$
- channel 5 AVHRR satellite brightness temperature T_5 , in $^{\circ}\text{C}$
- spatially averaged in situ air (or crop-top) temperature T_a , in $^{\circ}\text{C}$
- spatially averaged in situ vegetation temperature T_v , in $^{\circ}\text{C}$
- spatially averaged in situ ground temperature T_g , in $^{\circ}\text{C}$
- surface satellite zenith angle ϕ , in degrees
- solar zenith angle ψ in degrees.

The ATSR validation data-set contains four satellite brightness temperatures, the appropriate averaged in situ ground/vegetation/air temperature and the relevant angles. The in situ data are simple averages of the individual measurements at each site: 9 at Walpeup for the air (crop-top) and the bare soil surface, and 2 air temperatures; 5 vegetation/soil temperatures and 4 bare soil temperatures at the Hay site.

Some tables will not contain the solar zenith angle (nighttime data), and some tables will not contain the air (crop-top) or vegetation temperature.

The estimated instrumental rms accuracies of the data are ± 0.4 °C for AVHRR satellite brightness temperatures, ± 0.2 °C for ATSR brightness temperatures, and ± 0.2 °C for the in situ data. A quantitative error analysis for the satellite and in situ measurements has been carried out and is described in Prata (1994b). The analysis indicates that the largest absolute differences between the satellite and in situ data due to error sources should not exceed 3.3°C. Absolute differences less than 0.4°C are indistinguishable from the inherent instrument noise.

The times given are the satellite overpass time for the pixel closest to the field site. The in situ data were obtained within 3 minutes of this time, except for the ATSR validation data at Walpeup for which the data are interpolated from measurements made within 1 hour of the ATSR overpass time.

4.1 Walpeup validation data-sets

Tables 4-11 present the validation data for the Walpeup site. Table 4 lists the data for the

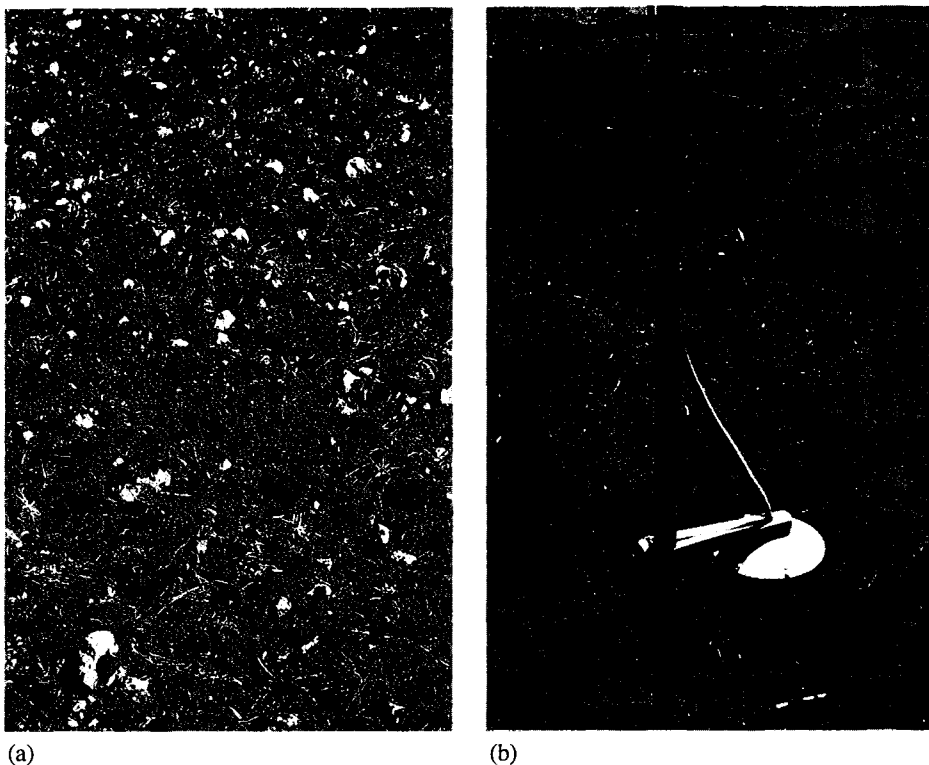


Figure 4. (a) Bare soil surface (ploughed field) at Walpeup, in March, 1990. (b) Temperature transducer on the sandy soil at Walpeup during March, 1990. The transducer may be seen at the base of the aluminium pole that was used for mounting the sensor to measure crop-top temperatures in the wheat crop (see Figures 5(b) and 6(b)).

field site when it was bare. Figure 4(a) shows the appearance of the surface at this time and Figure 4(b) shows one of the sensors placed in the sandy soil.

Tables 5-6 list the data for the field site when it was planted to a crop of wheat. The data are for a period when the crop was green in colour and the canopy cover was incomplete. Figures 5(a) and (b) show the canopy cover and the sensor placement at one of the eight "satellite" sites. Tables 7-8 list data for the wheat crop when at full cover (yellow in colour). Figures 6(a) and (b) show the canopy structure and sensor placement. Finally, Tables 9-11 list data for the period 28 August 1991 to 30 May 1992, when the field was lying fallow.

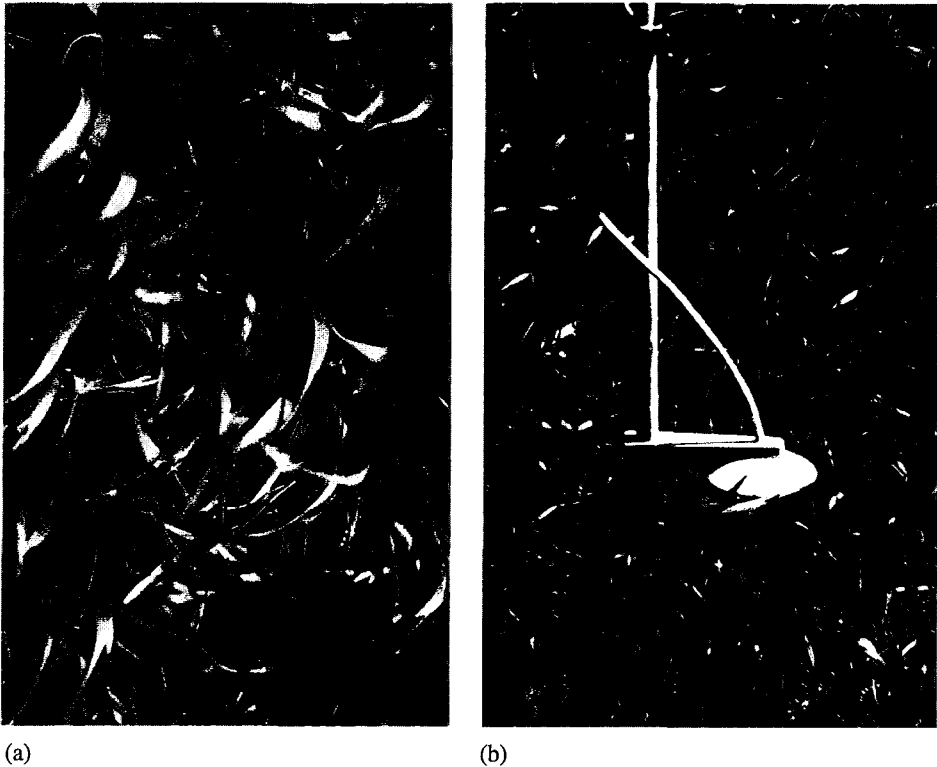


Figure 5. (a) Canopy cover at Walpeup when the field was sown to wheat during August 1990. (b) Temperature transducer measuring temperatures at the top of the growing wheat crop.

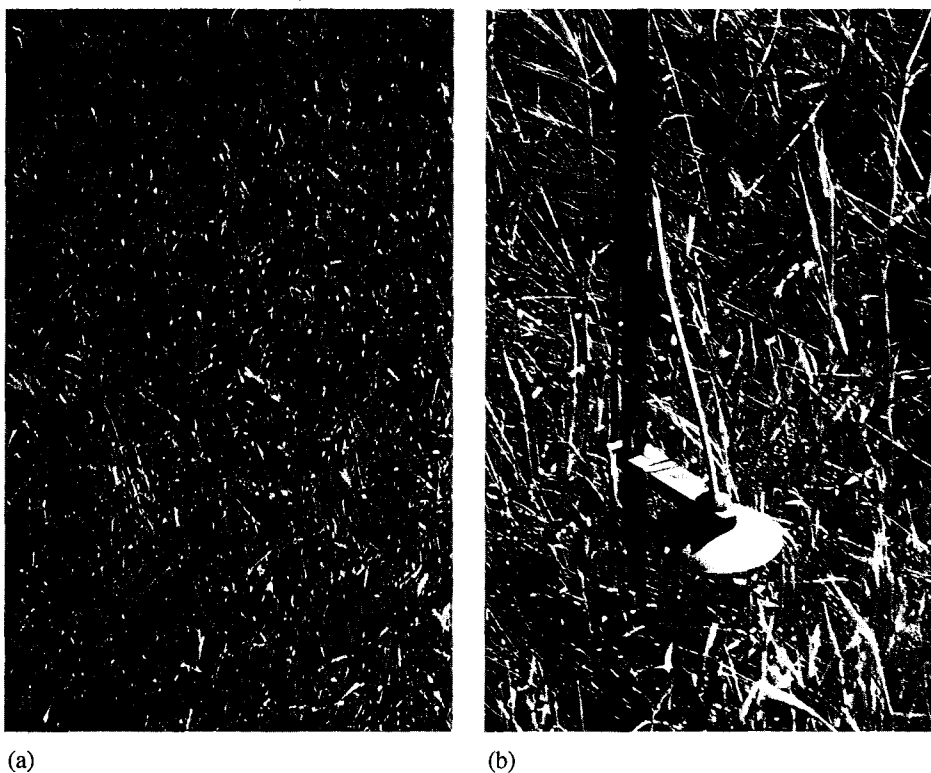


Figure 6. (a) Canopy structure of the wheat crop at Walpeup just prior to harvesting during November 1990. (b) Temperature transducer measuring temperatures at the top of the mature wheat crop.

4.2 Hay validation data-sets

The Hay validation data-sets are contained in Tables 12-16. The field site is used for grazing and no crops are planted. The vegetation goes through a natural cycle of growth during wet periods and senescence during dry spells (usually during the summer months). The site is not irrigated. Figure 7 shows one of the measurement locations on the Uardry site and gives a good indication of the type and structure of vegetation at the field site for most of the period starting in July 1992 to the present (April, 1994). Figures 8(a), (b) and (c) show the placement of sensors on the ground at three different locations at the Uardry site.

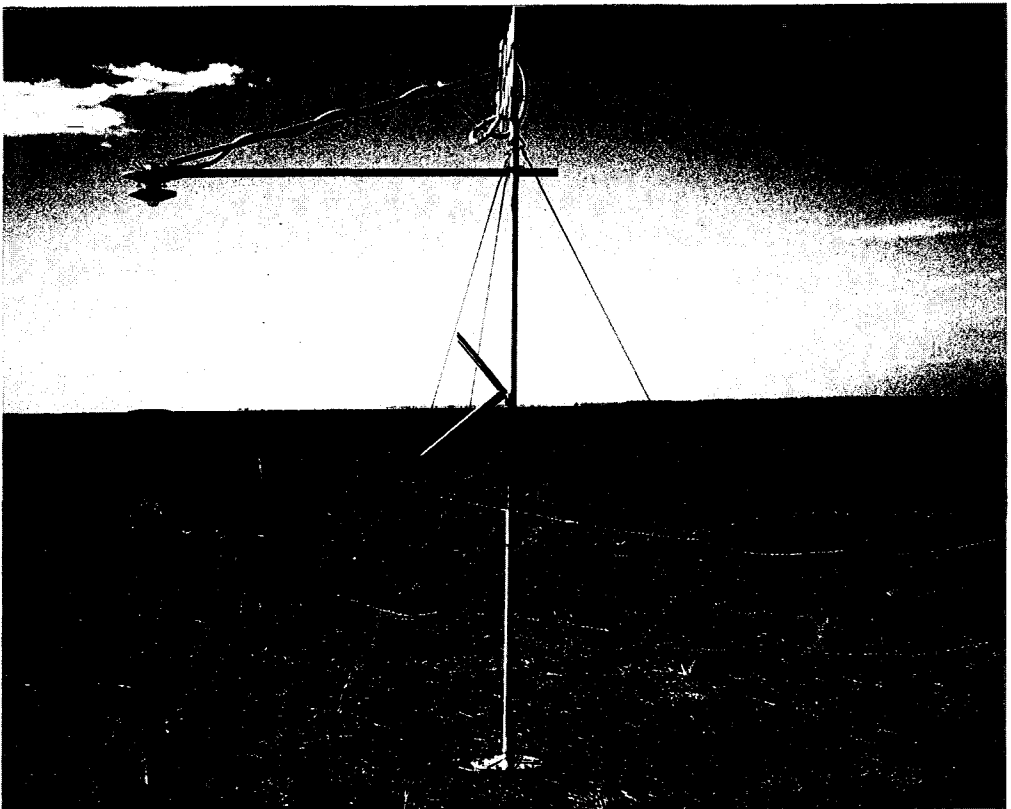


Figure 7. Photograph of one of the measurement stations at the Uardry field site during July, 1992.

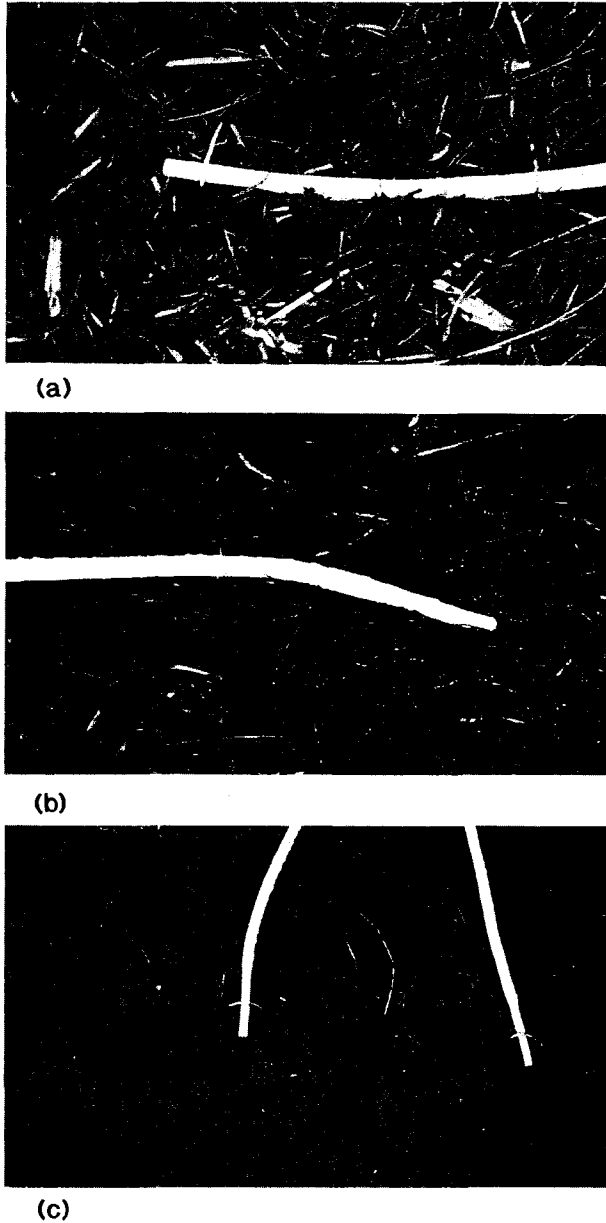


Figure 8. Photographs of the sensor placements at three measurement locations at the Uardry field site, Hay. (a) and (b) sensors in sparse vegetation, (c) sensors on bare ground.

4.3 ATSR validation data-sets

The ATSR is a conically scanning radiometer which permits two views of the same target on the earth's surface separated in time by about 140 s. These views are referred to here as the nadir view and forward view. The actual surface zenith angles vary with distance from the nadir across the scan. At the subsatellite point these angles are 0° and 55° . Figure 9 shows the variation of the surface zenith angle with distance across the scan.

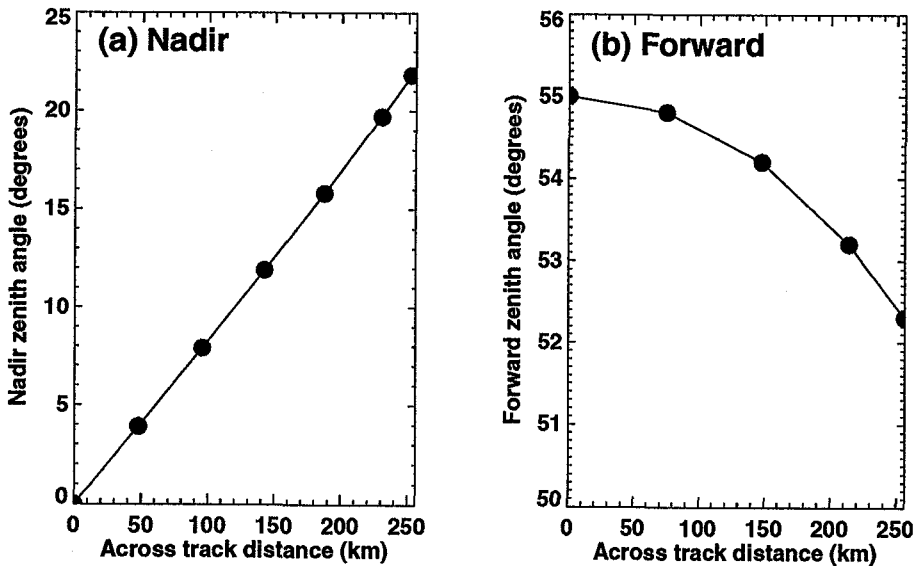


Figure 9. (a) Variation of surface zenith angle with distance across the scan (measured from the subsatellite point) for pixels on the nadir image. (b) Variation of surface zenith angle with distance across the scan (measured from the subsatellite point) for pixels on the forward image.

Two tables of ATSR validation data are included here. Table 17 lists the data for the Walpeup site in September and October 1991 when the field was fallow, and Table 18 lists data for the Hay site. Note that the in situ data at Walpeup were not synchronised with the ATSR overpass time, so that the values shown are interpolated values. Since most of the data are for clear periods during the nighttime, the error introduced due to this interpolation is small.

The ATSR data are preprocessed at the Rutherford Appleton Laboratory, which provides products consisting of calibrated brightness temperatures for the thermal channels and digital count values for the $1.6 \mu\text{m}$ channel. The maximum temperature that can be recorded in the $11 \mu\text{m}$ nadir channel appears to be 38.95°C (312.10 K). This restriction has limited the number of validation data points, particularly during the summer months when experience with AVHRR data has shown that $11 \mu\text{m}$ temperatures can exceed 50°C . All data (nadir and forward) are

navigated onto an equispaced grid in units of kilometres across the scan and along the track. The product sizes are 512 km x 512 km blocks for each image. Further details concerning the ATSR may be found in Delderfield et al. (1986). The ATSR scan geometry is described in Prata et al. (1989) and O'Brien and Prata (1990), and the data processing scheme is described by Bailey (1993).

Figure 10 shows an ATSR 1.6 μm relative reflectance image of the region of Victoria and NSW which includes both the Walpeup and Hay field sites, and demonstrates that for this image, the navigational accuracy is as good as that for the AVHRR (≈ 1 km).

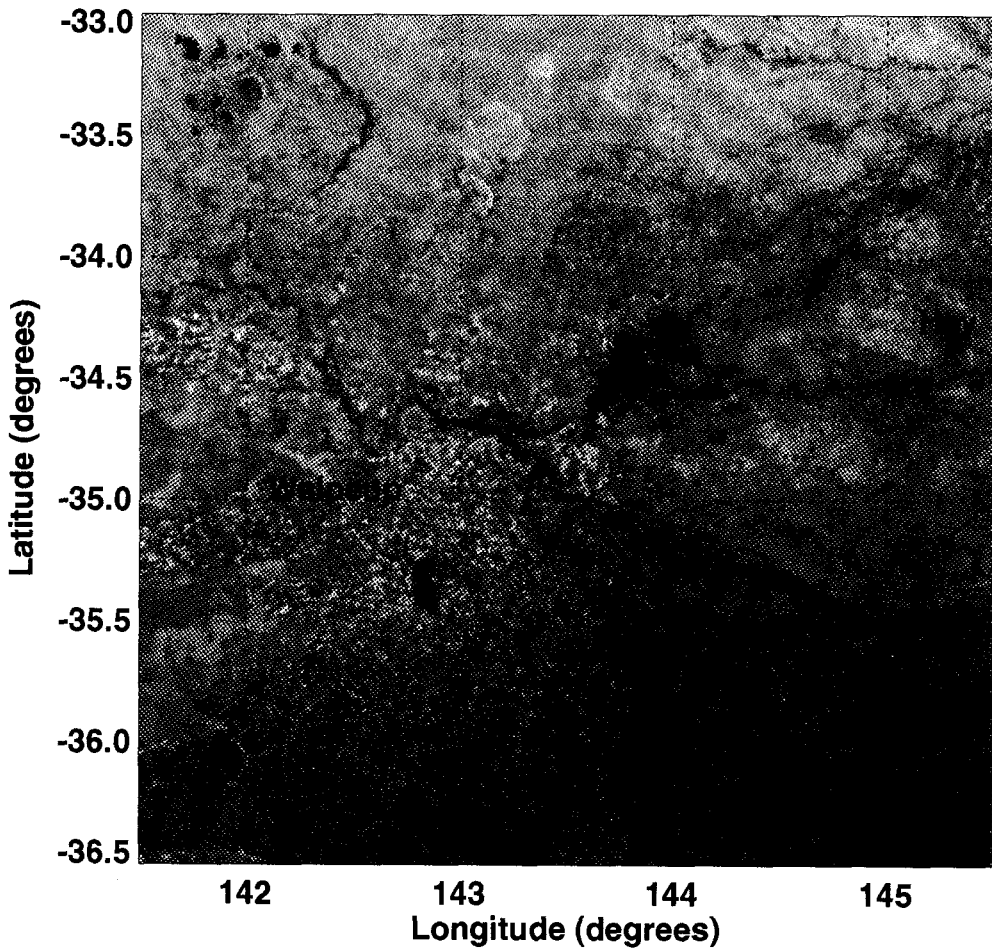


Figure 10. ATSR 1.6 μm relative reflectance (arbitrary units) satellite image of Victoria and southern New South Wales showing the locations of the field sites.

4.4 Atmospheric parameters

Users of these validation data will find it useful to have coincident atmospheric profile data. Such data are not available. However, monthly mean climatological data are available. Rather than provide tables of the profiles, some data reduction has been performed using LOWTRAN-7, and two tables are provided containing monthly mean values of the temperature of the lowest profile level, atmospheric transmittances for AVHRR channels 4 and 5 (nadir), the γ parameter, the downwelling and upwelling radiances for channels 4 and 5, and the total precipitable water. The derived parameters are defined by the following equations:

atmospheric transmittances for AVHRR channel i

$$\tau_i = \frac{\int_{\lambda_1}^{\lambda_2} \tau_s(p_s; p_{top}, \lambda) F_i(\lambda) d\lambda}{\int_{\lambda_1}^{\lambda_2} F_i(\lambda) d\lambda}, \quad (1)$$

$$\tau_{s, gas}(p_s; p, \lambda) = \exp \left[- \int_{p_s}^p k_{gas}(p', T) \rho_{gas}(p') \sec \theta dp' \right], \quad (2)$$

$$\tau_s(p_s; p_{top}, \lambda) = \prod_n \tau_{s, n}(p_s; p_{top}, \lambda), \quad (3)$$

γ parameter

$$\gamma_{ij} = \frac{1 - \tau_i}{\tau_i - \tau_j}, \quad (4)$$

atmospheric downwelling radiance for channel i

$$R_{i\downarrow} = \frac{\int_{p_{top}}^{p_s} \int_{\lambda_1}^{\lambda_2} B_i[T(p)] \frac{\partial \tau_s(p_{top}; p, \lambda)}{\partial p} dp F_i(\lambda) d\lambda}{\int_{\lambda_1}^{\lambda_2} F_i(\lambda) d\lambda}. \quad (5)$$

The atmospheric upwelling radiance $R_{i\uparrow}$ is defined in an analogous way to (5).

The precipitable water is defined as

$$PW = -\frac{1}{g} \int_{p_s}^{p_{top}} \frac{\rho_{wv}}{\rho_{wv} + \rho_{air}} dp. \quad (6)$$

The channel number is i , with response function $F(\lambda)$, λ is wavelength, λ_1 is the short wavelength cut-off, λ_2 is the long wavelength cut-off, θ is the zenith angle for incident radiation, $B_\lambda[T]$ is the Planck function, p is pressure, p_{top} is the pressure corresponding to the highest level in the profile, p_s is the pressure corresponding to the lowest level, $T(p)$ is the temperature profile, k_{gas} is the absorption coefficient for a particular gas, ρ is the absorber density (ρ_{wv} is the density of water vapour), n is the number of gases contributing in the waveband ($\lambda_1 \rightarrow \lambda_2$), $R_i\downarrow$, $R_i\uparrow$ are the atmospheric downwelling and upwelling radiances, respectively, τ_i is the total atmospheric transmittance integrated over the filter response function, g is the acceleration due to gravity, and PW is the total precipitable water in units of $g\text{ cm}^{-2}$.

These data may be used to solve for the surface temperature, T_s from a radiance measurement, R_i , using the radiative transfer equation

$$R_i = \tau_i R_{s,i} + R_i\uparrow \quad (7)$$

where the surface leaving radiance in channel i is given by

$$R_{s,i} = \epsilon_i B_i[T_s] + (1 - \epsilon_i) R_i\downarrow. \quad (8)$$

Table 19 contains data for the Walpeup site, while Table 20 contains the data for the Hay site. The tabulated data are interpolated from a set of 23 Bureau of Meteorology upper-air stations (Maher and Lee, 1977; see Prata, 1994a for further details).

4.5 Emissivity data

A few laboratory emissivity measurements were made for the soils found at Walpeup and Hay. These measurements were made using the 'gold-box' method described by Buettner and Kern (1965) and are directional emissivities (vertical only). Values for wheat (growing and senesced) are included, based on the measurements of Huband and Monteith (1986). The emissivity values for Walpeup and Hay are listed in Table 21.

Acknowledgements

The field work described in this paper would not have been possible without the cooperation of John Symes and Chris Bowman who allowed us unrestricted access to the properties at Walpeup and Uardry. I thank them for their assistance.

Graham Rutter, Bob Cechet and Richard Mieczko of the CSIRO Division of Atmospheric Research provided many hours of help setting up and maintaining the field equipment. Janice Bathols (DAR) assisted with the AVHRR data processing and helped with the difficult task of accurately navigating the imagery. The Division's mechanical and electronic engineers, Reg Henry, Ron Hill, Craig Smith, John Bennett, Matt Fenwick, and Bernie Petraitis built, tested, and helped deploy the instrumentation at Walpeup and Uardry.

The ATSR data are used courtesy of the European Space Agency, and were supplied by the Rutherford Appleton Laboratory.

References

- Bailey, P. (1993). SADIST Products (Version 500), *Space Eng. Dept., Rutherford Appleton Laboratory*, Didcot, England, 60pp.
- Buettner, K. J., and C. D. Kern (1965). The determination of infrared emissivities for terrestrial surfaces. *J. Geophys. Res.*, **70**, 1329-1337.
- Climate averages Australia (1988). Bureau of Meteorology, Department of Administrative Services, *Australian Government Publishing Service*, Canberra, Australia, 532pp.
- Delderfield, et al., (1986). The Along-Track Scanning Radiometer for ERS-1. In *Instrumentation for Optical Remote Sensing from Space*, J. S. Seeley, J. W. Lear, A. Monfils and S. L. Russak, Eds., *Proc. SPIE*, 589, 114-120.
- Huband, N. D. S., and J. L. Monteith (1986). Radiative temperature and energy balance of wheat canopy. Part I: Comparison of radiative and aerodynamic canopy temperature, *Boundary-layer Meteorol.*, **36**, 1-17.
- Maher, J.V., and D. M. Lee (1977). Upper air statistics, Australia, Surface to 5 mb, 1957-1975, Meteorological Summary, Bureau of Meteorology, *Australian Government Publishing Service*, Canberra, Australia, 202pp.
- O'Brien, D. M., and A. J. Prata (1990). Navigation of ERS-1 Along-Track Scanning Radiometer (ATSR) images, *ESA Journal*, **14**, 447-465.
- Planet, W. (1988). Data extraction and calibration of TIROS-N/NOAA radiometers, *NOAA Tech. Memo., NESS 107 Rev. 1*, 58 pp, U.S. Dept. of Commerce, NOAA/NESDIS, Washington, D. C.
- Prata, A. J., R. P. Cechet, I. J. Barton and D. T. Llewellyn-Jones (1990). The Along Track Scanning Radiometer for ERS-1- Scan geometry and data simulation, *IEEE Trans. Geosci. Rem. Sens.*, **28**, 3-13.
- Prata, A. J., D. M. O'Brien, D. M., and C. M. R. Platt (1990). Algorithms for deriving land surface temperature from satellite measurements, *Proc. of the 5th Australasian Remote Sens. Conf.*, 256-266, Perth, Western Australia, 8-12 October 1990.
- Prata, A. J., J. Bennett, M. Fenwick, D. Graetz, R. Mitchell, B. Petraitis and G. Rutter (1992). Validating remotely sensed land surface temperatures, *Proc. of the 6th Australasian Remote Sens. Conf.*, **3**, 241-249, Wellington, New Zealand, 2-6 November, 1992.
- Prata, A. J. (1993). Land surface temperatures derived from the AVHRR and ATSR, 1, Theory, *J. Geophys. Res.*, **98**, 16,689-16,702.
- Prata, A. J. (1994a). Land surface temperature derivation from satellites, *Adv. Space Res.*, **14**(3), 15-26.
- Prata, A. J. (1994b). Land surface temperatures derived from the AVHRR and ATSR, 2, Experimental results and validation of AVHRR algorithms, *J. Geophys. Res.*, **99**, 13,025-13,058.

Tables

Table 1: Mean annual climatological data for the Walpeup and Hay field sites. The data for Hay are from the Hay Post Office, about 40 km distant from the field site while those for Walpeup are from the Mallee Research Station approximately 8 km distant from the field site. (Adapted from *Climatic averages Australia*, 1988.)

Parameter	Walpeup	Hay
Mean annual precipitation (mm)	343	365
Rain days	95	65
Daily maximum air temperature (°C)	23.2	24.1
Daily minimum air temperature (°C)	9.9	10.4
9am mean temperature dry-bulb (°C)	15	15.8
9am Humidity (%)	64	63
3pm mean temperature dry-bulb (°C)	22	22.9
3pm Humidity (%)	39	40
Elevation (m)	107	94

Table 2: Configuration and location of the CSIDAT radio hub at Hay, NSW. The symbols have the following meanings:- A - anemometer, T - temperature transducer (a - air, g - ground), Pnnn - pyranometer (↑ - upward looking, ↓ - downward looking) and E - Eppley pyrgeometer. Accurate locations of the equipment (± 100 m) were obtained using a hand-held GPS receiver.

Site No.	Latitude	Longitude	Instrument		Heights (m)	
			Channel 1	Channel 2		
0	34°23.76'	145°18.18'	Tg	Ta	0.00	1.00
1	34°23.66'	145°18.21'	Tg	A10	0.00	3.00
2	34°23.53'	145°18.53'	Tg	A8	0.00	3.00
3	34°23.35'	145°18.30'	Tg	P421↓	0.00	2.47
4	34°23.27'	145°18.33'	Tg	Ta	0.00	1.00
5	34°23.45'	145°17.97'	Tg	Tg	0.00	0.00
6	34°23.50'	145°18.42'	Tg	P419↓	0.00	2.43
7	34°23.50'	145°18.11'	Tg	P420↓	0.00	2.43
8	34°23.50'	145°18.28'	E	P418↑	4.00	4.00

Table 3: Characteristics of the AVHRR and ATSR relevant to the estimation of surface temperatures. The approximate pixel sizes are given for the nadir view and for the view with the largest scan angle. Dimensions are given as across track diameter by along track diameter.

Channel	Central wavelength (μm)	NE Δ T ($^{\circ}\text{C}$)	Resolution (km)	
			nadir	$\pm 55.4^{\circ}$
AVHRR				
3	3.7	0.30	1.1x1.1	6.8x2.4
4	10.8	0.12	1.1x1.1	6.8x2.4
5	11.9	0.12	1.1x1.1	6.8x2.4
			nadir	forward (47.5°)
ATSR				
1	3.7	<0.10	1.2x1.0	1.5x3.0
2	10.8	0.03	1.2x1.0	1.5x3.0
3	11.9	0.03	1.2x1.0	1.5x3.0

Table 4: AVHRR brightness temperatures ($^{\circ}\text{C}$) and in situ validation temperatures ($^{\circ}\text{C}$) for the bare soil surface at the Walpeup field site. In situ temperatures are given for the sensor covered by foil ($T_g(\text{F})$) and the black coloured sensor ($T_g(\text{B})$). The date, time (hours:minutes, Local Time = UT+10), surface satellite zenith angle (ϕ in degrees) and solar zenith angle (ψ in degrees) are given for the pixel closest to the field site.

D/M/Y	Time (UT)	T_3	T_4	T_5	$T_g(\text{F})$	$T_g(\text{B})$	ϕ	ψ
<i>Daytime data</i>								
04/04/90	05:32	37.62	31.08	28.86	36.32	37.17	45.3	60.0
05/04/90	05:21	42.21	32.40	28.29	42.96	41.25	33.5	58.4
06/04/90	05:11	40.69	33.33	30.33	39.97	41.23	18.5	57.1
07/04/90	05:00	38.63	32.06	30.54	35.26	36.78	1.0	55.6
09/04/90	04:30	39.94	33.18	31.63	36.98	38.90	32.3	51.8
12/04/90	04:07	37.93	29.08	26.27	36.10	37.51	61.7	49.9
15/04/90	05:11	28.66	18.06	16.36	24.07	25.36	22.6	60.0
16/04/90	04:55	32.00	24.10	23.24	27.92	28.14	5.6	57.8
22/04/90	03:50	28.28	18.58	17.18	22.22	22.88	66.3	51.4
22/04/90	05:40	25.88	19.26	18.62	21.68	21.27	50.0	66.8
23/04/90	05:19	26.77	16.91	14.93	23.51	24.62	31.8	63.4
25/04/90	04:58	26.70	18.88	17.84	23.83	23.88	9.8	61.0
20/05/90	05:27	19.90	14.49	14.01	18.36	19.77	47.0	70.9
<i>Nighttime data</i>								
05/04/90	15:03	11.90	12.84	12.11	17.33	17.16	66.0	—
05/04/90	16:45	11.53	12.68	12.44	16.37	16.27	49.2	—
06/04/90	16:30	9.00	7.88	7.18	12.87	12.80	38.0	—
07/04/90	16:25	8.06	8.80	8.63	11.91	11.74	23.7	—
09/04/90	16:15	7.60	6.67	6.24	12.24	12.12	11.5	—
16/04/90	16:18	5.53	6.89	7.29	9.51	9.47	27.6	—
23/04/90	15:09	8.80	10.38	10.08	14.41	15.25	53.6	—
25/04/90	16:21	4.71	6.12	6.57	8.92	9.05	31.1	—
26/04/90	16:10	2.86	3.73	4.00	6.60	6.67	15.2	—
17/05/90	15:43	4.83	5.44	5.43	7.18	7.46	66.0	—
18/05/90	15:32	1.27	2.48	2.96	4.88	5.08	41.9	—
19/05/90	15:22	1.65	2.78	3.16	4.74	4.66	51.7	—
20/05/90	15:51	0.02	0.70	1.20	4.00	3.91	23.0	—
30/05/90	16:44	5.17	6.32	6.21	9.35	9.40	53.4	—
03/06/90	15:59	3.54	4.30	4.66	7.22	7.25	9.5	—
04/06/90	15:48	2.42	3.48	3.84	5.86	5.91	19.5	—
05/06/90	15:38	1.64	2.44	3.03	4.51	4.50	34.0	—

Table 5: Daytime AVHRR brightness temperatures ($^{\circ}\text{C}$) and in situ validation temperatures ($^{\circ}\text{C}$) for the growing wheat crop at Walpeup. The date, time (hours:minutes), satellite surface zenith angle (ϕ in degrees) and the solar zenith angle (ψ in degrees) are given for the pixel closest to the field site.

D/M/Y	Time (UT)	T_3	T_4	T_5	T_a	T_g	ϕ	ψ
22/08/90	05:08	11.33	9.39	9.04	10.33	12.57	13.6	60.8
23/08/90	04:55	15.89	10.38	9.95	13.38	14.97	4.6	58.6
26/08/90	04:22	20.35	17.18	16.59	16.85	19.86	48.3	53.3
29/08/90	05:30	16.05	13.91	12.64	17.10	21.51	27.1	62.8
30/08/90	05:20	18.98	15.81	14.96	18.69	18.32	19.4	60.9
01/09/90	04:56	24.48	14.00	12.16	18.70	19.67	2.5	56.6
03/09/90	04:34	16.81	13.07	11.97	14.79	16.49	34.0	52.9
14/09/90	04:16	22.80	19.10	18.24	19.15	22.04	56.5	47.5
15/09/90	04:03	24.12	20.45	18.95	21.71	24.02	62.8	45.4
16/09/90	05:33	27.04	23.05	21.99	22.00	26.16	46.3	59.6
19/09/90	05:00	32.83	28.47	26.89	28.61	31.80	1.5	53.2
20/09/90	04:49	33.20	29.73	28.18	28.25	31.73	16.8	51.1
21/09/90	04:38	30.27	26.43	25.29	22.82	27.51	32.8	49.0
22/09/90	04:27	31.91	25.68	23.81	25.22	29.41	45.8	47.0
23/09/90	04:16	31.65	27.56	26.85	25.87	28.65	55.1	45.1
28/09/90	05:02	24.14	21.03	19.62	24.54	26.14	3.1	51.6
30/09/90	04:40	35.77	28.54	26.78	29.60	31.66	31.8	47.3
02/10/90	06:01	29.73	24.88	22.63	26.64	28.64	46.3	62.0
03/10/90	04:08	43.81	25.51	23.26	28.04	33.91	61.5	41.3

Table 6: Nighttime AVHRR brightness temperatures ($^{\circ}\text{C}$) and in situ validation temperatures ($^{\circ}\text{C}$) for the growing wheat crop at Walpeup. The date, time (hours:minutes) and satellite surface zenith angle (ϕ in degrees) are given for the pixel closest to the field site.

D/M/Y	Time (UT)	T_3	T_4	T_5	T_a	T_g	ϕ
15/08/90	16:08	3.44	3.85	3.85	3.98	5.19	4.0
16/08/90	15:56	1.51	2.14	2.20	3.28	4.42	19.7
17/08/90	15:45	-0.23	0.46	0.74	-0.74	3.49	35.3
21/08/90	16:42	2.49	2.98	2.71	4.45	5.50	46.6
22/08/90	15:31	2.24	2.73	2.82	4.28	5.06	34.5
23/08/90	16:20	3.12	5.65	5.18	7.07	9.55	18.8
25/08/90	15:58	1.04	1.95	2.10	1.15	4.30	17.3
26/08/90	15:47	-1.24	-0.68	-0.70	-0.55	2.16	32.5
29/08/90	15:14	0.97	2.16	2.35	1.96	5.55	61.1
29/08/90	16:56	0.64	1.70	2.01	1.60	5.20	56.2
31/08/90	16:33	1.56	2.02	2.21	-0.09	4.02	35.6
01/09/90	16:21	1.42	2.10	2.18	0.92	4.39	22.0
03/09/90	15:59	5.21	6.10	5.62	8.54	10.10	15.2
04/09/90	15:44	2.43	3.61	3.79	5.47	8.07	30.9
13/09/90	15:50	2.04	2.69	2.78	2.00	5.82	29.4
14/09/90	15:39	3.22	3.68	3.75	3.49	7.21	42.3
15/09/90	15:28	0.76	1.79	2.10	1.86	6.85	52.1
18/09/90	16:36	5.84	6.02	6.43	7.25	9.09	38.5
19/09/90	16:25	9.18	6.17	4.99	12.72	13.50	51.3
20/09/90	16:14	6.29	7.01	6.98	7.62	10.35	6.7
21/09/90	16:03	0.36	0.05	-0.02	-0.50	3.62	11.6
26/09/90	16:49	0.52	1.86	1.80	0.09	5.56	50.6
26/09/90	16:48	2.03	3.30	3.18	4.86	7.33	50.9
28/09/90	16:27	2.96	3.97	4.11	2.10	7.04	25.4
29/09/90	16:16	3.56	4.55	4.85	0.69	6.49	8.3
30/09/90	16:04	3.86	4.48	4.94	1.74	6.63	10.1
01/10/90	15:53	3.58	5.09	5.23	4.16	9.18	27.0
02/10/90	15:42	3.59	4.97	5.00	2.33	8.73	37.0
05/10/90	15:10	4.00	4.54	5.12	6.12	8.38	62.9
08/10/90	16:17	3.98	4.25	4.43	2.48	7.66	12.1
09/10/90	16:06	3.11	4.39	4.73	2.44	7.60	5.6
11/10/90	15:44	4.82	5.38	5.43	3.69	8.62	35.9

Table 7: Daytime AVHRR brightness temperatures ($^{\circ}\text{C}$) and in situ validation temperatures ($^{\circ}\text{C}$) for the mature wheat crop at Walpeup. The date, time (hours:minutes), satellite surface zenith angle (ϕ in degrees) and solar zenith angle (ψ in degrees) are given for the pixel closest to the field site.

D/M/Y	Time (UT)	T_3	T_4	T_5	T_a	T_g	ϕ	ψ
22/10/90	04:06	30.11	24.65	20.55	26.85	37.11	67.4	36.5
23/10/90	05:35	33.13	28.74	26.87	28.83	35.26	38.4	53.2
24/10/90	05:24	37.38	33.50	31.58	32.93	39.70	24.0	50.9
25/10/90	05:15	47.70	37.90	36.02	35.66	43.03	6.6	48.9
26/10/90	05:04	16.52	45.03	44.06	37.96	46.13	12.1	46.5
28/10/90	04:39	45.54	41.68	39.57	41.60	47.57	42.5	41.3
29/10/90	04:28	47.23	40.62	37.75	41.44	52.86	52.9	39.0
01/11/90	05:38	36.36	29.66	25.88	30.04	39.21	38.9	52.3
02/11/90	05:27	45.53	31.09	27.34	34.09	44.99	24.6	49.9
04/11/90	05:05	43.91	39.27	36.11	37.42	45.44	11.3	45.1
05/11/90	04:55	48.10	42.54	39.48	41.29	47.79	28.4	43.0
11/11/90	05:21	39.62	33.21	31.69	33.20	40.65	23.9	47.2
12/11/90	05:08	41.94	31.12	29.00	31.95	40.76	7.1	44.4
14/11/90	04:55	44.04	37.90	35.40	35.94	46.75	27.8	41.4
15/11/90	04:44	43.43	39.09	36.89	35.88	47.96	41.6	39.0
16/11/90	04:33	42.60	35.72	33.75	33.55	42.66	52.3	36.7
18/11/90	05:55	41.49	32.76	31.15	30.95	40.68	50.1	53.0
21/11/90	05:18	43.55	31.27	29.14	31.17	35.75	8.2	45.0
23/11/90	04:56	43.87	32.09	31.50	27.43	37.24	27.4	40.1
24/11/90	04:45	44.96	37.39	34.75	35.15	45.20	41.3	37.8
25/11/90	04:34	43.79	36.64	34.14	35.18	44.61	51.9	35.4
25/11/90	06:14	38.68	29.57	26.99	32.17	37.64	64.6	55.9
26/11/90	04:23	44.60	33.94	29.32	38.66	47.00	60.0	33.0

Table 8: Nighttime AVHRR brightness temperatures ($^{\circ}\text{C}$) and in situ validation temperatures ($^{\circ}\text{C}$) for the mature wheat crop at Walpeup. The date, time (hours:minutes) and satellite surface zenith angle (ϕ in degrees) are given for the pixel closest to the field site.

D/M/Y	Time (UT)	T_3	T_4	T_5	T_a	T_g	ϕ
19/10/90	15:56	4.21	5.09	5.23	4.16	9.81	15.6
20/10/90	15:43	2.23	2.63	2.40	1.25	6.01	21.3
21/10/90	15:35	2.81	3.21	3.17	3.96	7.46	46.8
22/10/90	15:23	4.64	5.75	5.68	5.20	8.85	51.5
25/10/90	16:38	8.16	9.09	9.14	6.69	12.74	29.9
26/10/90	16:27	7.23	10.14	10.33	6.68	12.56	50.1
28/10/90	16:04	13.02	13.06	13.22	10.95	16.50	12.7
01/11/90	15:21	8.24	8.69	7.53	9.29	15.11	64.4
03/11/90	16:39	9.26	13.41	12.99	11.77	16.08	29.4
04/11/90	16:28	12.29	14.85	14.86	12.52	18.30	15.0
05/11/90	16:17	16.96	17.10	16.45	16.80	21.71	6.1
10/11/90	15:15	1.13	3.09	2.98	5.40	10.59	60.9
10/11/90	16:56	1.97	2.96	2.71	5.21	10.03	54.0
14/11/90	16:00	9.49	9.32	9.25	8.44	16.69	23.1
15/11/90	16:07	9.00	9.99	9.94	8.22	15.47	0.1
16/11/90	15:56	9.79	10.05	8.92	12.67	17.41	37.7
17/11/90	15:45	6.26	7.50	7.05	9.09	14.36	48.9
18/11/90	15:34	8.12	9.59	9.57	9.50	13.78	57.4
19/11/90	17:04	7.27	7.71	7.43	6.05	13.27	53.8
21/11/90	16:42	5.33	8.48	8.32	7.23	14.40	30.3
22/11/90	16:30	8.04	6.99	6.91	6.38	13.07	13.6
23/11/90	16:20	5.50	7.20	7.02	5.59	12.78	0.2
25/11/90	15:57	7.17	8.78	8.43	8.25	15.14	37.5

Table 9: Daytime NOAA-11 AVHRR brightness temperatures ($^{\circ}\text{C}$) and in situ validation temperatures ($^{\circ}\text{C}$) for the Walpeup site when the field was left fallow. The date, time (hours:minutes), satellite surface zenith angle (ϕ in degrees) and solar zenith angle (ψ in degrees) are given for the pixel closest to the field site.

D/M/Y	Time (UT)	T_3	T_4	T_5	T_g	T_v	ϕ	ψ
28/08/91	05:58	17.10	12.45	11.98	15.16	16.59	41.0	67.9
01/09/91	05:11	20.96	16.49	15.94	17.92	18.34	24.5	59.1
02/09/91	05:00	23.44	18.51	17.36	21.35	23.26	39.2	57.1
03/09/91	04:49	21.75	16.83	15.19	21.84	21.46	50.6	55.1
04/09/91	04:37	23.82	19.46	18.33	24.00	24.28	59.3	53.1
05/09/91	06:06	25.04	16.66	15.06	23.76	23.49	36.4	67.9
09/09/91	05:20	23.79	20.69	19.97	24.30	24.06	13.7	58.8
13/09/91	04:34	20.98	16.19	14.31	21.77	21.57	6.2	50.4
17/09/91	05:28	14.42	12.39	11.72	14.25	14.70	2.2	58.6
18/09/91	05:19	19.60	12.37	11.12	16.32	16.48	20.1	56.8
22/09/91	06:11	20.67	16.31	15.41	19.87	20.28	50.5	65.8
23/09/91	05:59	24.66	20.01	19.10	22.05	22.67	39.8	63.3
26/09/91	05:24	21.59	19.12	17.95	24.36	22.56	9.2	56.1
27/09/91	05:12	26.24	20.40	18.74	26.39	25.92	26.5	53.7
29/09/91	04:49	23.85	20.34	18.86	26.03	25.78	52.0	49.1
03/10/91	05:44	32.41	30.06	28.32	36.18	34.96	19.7	58.6
04/10/91	05:34	35.83	33.03	31.30	39.23	38.47	1.9	56.4
05/10/91	05:20	35.35	31.98	30.34	38.22	37.17	16.4	53.6
06/10/91	05:09	30.11	27.03	25.23	35.37	29.92	32.8	51.3
10/10/91	06:03	31.18	20.18	18.01	28.61	24.14	42.5	61.1
11/10/91	05:52	32.48	23.47	21.43	33.05	30.45	29.3	58.7
13/10/91	05:28	33.37	31.39	30.10	35.58	32.44	5.6	53.6
02/04/92	05:18	38.45	30.28	26.41	45.10	39.09	45.5	56.8
03/04/92	05:07	39.07	29.69	25.42	44.45	39.03	55.8	55.3
29/05/92	05:39	16.77	14.29	14.19	17.22	16.62	41.1	73.8
30/05/92	05:28	19.69	15.75	15.72	18.64	18.32	26.0	72.2

Table 10: Nighttime NOAA-11 AVHRR brightness temperatures ($^{\circ}\text{C}$) and in situ validation temperatures ($^{\circ}\text{C}$) for the Walpeup site when the field was left fallow. The date, time (hours:minutes), satellite surface zenith angle (ϕ in degrees) and solar zenith angle (ψ in degrees) are given for the pixel closest to the field site.

D/M/Y	Time (UT)	T_3	T_4	T_5	T_g	T_v	ϕ	ψ
28/08/91	15:53	2.05	2.74	2.08	6.09	5.26	59.6	—
02/09/91	16:25	2.66	3.60	3.86	5.21	4.91	18.0	—
03/09/91	16:13	1.63	2.54	2.96	5.04	1.29	33.3	—
04/09/91	16:02	2.84	3.90	4.19	4.47	2.47	45.5	—
05/09/91	15:50	4.19	5.29	6.00	5.42	2.40	54.8	—
10/09/91	16:33	3.89	4.77	4.57	7.50	6.25	6.8	—
11/09/91	16:21	1.23	1.88	1.91	5.13	1.86	23.8	—
15/09/91	17:16	7.41	8.60	8.36	13.14	11.23	48.9	—
16/09/91	17:07	5.29	5.02	4.49	9.46	7.26	36.7	—
18/09/91	16:42	3.08	2.83	2.82	6.84	4.24	2.2	—
19/09/91	16:30	0.80	1.02	1.66	5.19	0.48	17.0	—
20/09/91	16:18	4.30	3.36	3.35	9.09	8.11	33.3	—
22/09/91	15:55	0.61	1.89	2.45	5.55	0.30	55.3	—
22/09/91	17:37	-0.37	0.49	1.03	3.93	-1.26	62.7	—
26/09/91	16:46	1.58	2.28	2.95	6.54	0.83	14.1	—
30/09/91	16:03	7.64	7.47	8.12	12.10	8.40	49.9	—
02/10/91	15:40	8.04	7.43	7.15	12.31	9.55	65.0	—
06/10/91	16:34	3.79	4.83	5.16	10.69	4.18	12.9	—
07/10/91	16:22	6.81	7.24	7.04	12.60	9.32	30.0	—
08/10/91	16:11	1.12	2.15	2.21	9.63	3.95	43.5	—
09/10/91	15:59	2.79	4.34	4.52	10.28	4.82	53.6	—
09/10/91	17:41	3.30	4.15	4.38	9.45	3.87	64.1	—
10/10/91	15:48	4.09	4.80	5.53	10.75	4.72	61.2	—
13/10/91	16:54	5.16	6.13	6.78	9.82	3.53	17.9	—
15/10/91	16:31	7.43	7.06	6.29	13.81	8.37	20.2	—
16/10/91	16:19	1.75	2.44	2.87	7.44	-0.18	35.9	—
22/10/91	16:49	6.57	6.84	7.41	12.58	5.90	10.1	—
23/10/91	16:37	7.53	8.01	8.64	12.90	6.97	9.6	—
29/10/91	17:08	12.50	12.56	12.41	17.69	11.67	36.9	—
30/10/91	16:57	7.53	7.44	7.91	11.95	7.13	20.8	—
31/10/91	16:45	5.12	5.47	5.91	10.18	5.29	1.7	—
02/04/92	16:41	14.01	14.89	14.52	17.33	15.81	25.9	—
29/05/92	17:03	-0.64	0.58	1.21	1.16	1.13	2.0	—
30/05/92	16:51	1.46	1.88	2.73	1.51	1.21	20.2	—

Table 11: Evening NOAA-12 AVHRR brightness temperatures ($^{\circ}\text{C}$) and in situ validation temperatures ($^{\circ}\text{C}$) for the Walpeup site when the field was left fallow. The date, time (hours:minutes), satellite surface zenith angle (ϕ in degrees) and solar zenith angle (ψ in degrees) are given for the pixel closest to the field site.

D/M/Y	Time (UT)	T_3	T_4	T_5	T_g	T_v	ϕ	ψ
28/08/91	10:04	4.14	4.20	4.20	4.74	5.06	24.7	—
02/09/91	10:00	4.92	5.76	5.70	8.39	8.96	30.1	—
03/09/91	09:40	5.35	6.71	6.42	11.11	8.28	52.9	—
10/09/91	10:34	3.86	5.12	4.66	8.44	7.59	24.3	—
17/09/91	09:49	4.91	4.83	3.64	10.71	10.37	45.0	—
18/09/91	11:09	2.29	3.79	3.39	9.26	7.26	58.6	—
19/09/91	10:48	1.44	2.41	2.17	8.45	3.90	40.9	—
22/09/91	09:45	5.66	5.83	5.63	11.21	7.61	48.9	—
26/09/91	10:02	5.43	7.11	6.82	13.55	8.67	29.3	—
30/09/91	10:19	9.11	10.67	10.64	14.64	10.83	2.2	—
07/10/91	11:14	7.43	7.51	6.24	14.74	11.20	61.4	—
08/10/91	10:53	4.82	6.00	4.69	13.84	9.22	45.6	—
09/10/91	10:32	9.22	10.09	9.48	15.22	11.40	19.2	—
10/10/91	10:11	8.85	9.74	9.37	14.37	10.06	16.0	—
13/10/91	10:49	7.54	9.11	9.19	14.74	7.82	41.3	—
14/10/91	10:30	15.61	16.56	16.19	20.68	16.96	12.5	—
22/10/91	09:22	10.18	11.59	10.71	18.87	13.44	66.0	—
23/10/91	10:40	10.50	11.70	11.18	16.99	11.38	31.2	—
24/10/91	10:20	12.74	12.99	11.76	19.84	15.45	1.9	—
31/10/91	09:33	9.38	10.03	9.45	15.61	10.80	58.5	—
02/04/92	10:38	13.19	14.57	14.47	17.25	17.36	24.5	—
20/04/92	10:57	5.46	6.85	6.93	9.75	9.71	46.7	—
21/04/92	10:36	4.45	6.16	6.12	8.65	8.05	20.8	—
29/05/92	10:29	2.77	3.43	3.94	4.67	4.69	10.6	—
30/05/92	10:08	3.54	4.41	4.96	6.15	6.01	23.6	—

Table 12 Morning NOAA-12 AVHRR brightness temperatures ($^{\circ}\text{C}$) and *in situ* validation temperatures ($^{\circ}\text{C}$) for the Walpeup site when the field was left fallow. The date, time (hours:minutes), satellite surface zenith angle (ϕ in degrees) and solar zenith angle (ψ in degrees) are given for the pixel closest to the field site.

D/M/Y	Time(UT)	T_3	T_4	T_5	T_g	T_v	ϕ	ψ
28/08/91	21:25	4.97	4.04	4.26	5.33	5.35	9.0	82.3
31/08/91	22:02	5.57	3.50	3.18	3.38	7.01	45.5	74.3
02/09/91	21:21	3.62	3.97	3.77	6.38	4.49	18.7	83.3
03/09/91	21:00	0.37	1.70	1.90	4.14	-0.05	45.3	87.2
05/09/91	21:59	9.17	7.48	7.56	10.26	6.25	40.4	75.0
07/09/91	21:17	7.68	7.73	7.46	11.24	9.30	24.6	82.6
08/09/91	20:57	1.63	2.19	2.29	4.94	-0.12	49.0	86.5
10/09/91	21:55	14.06	3.62	2.55	6.78	6.68	35.7	74.3
11/09/91	21:34	1.49	3.91	3.33	7.24	6.57	3.6	71.2
15/09/91	21:51	11.40	10.78	10.23	14.05	15.29	30.6	73.5
17/09/91	21:09	7.02	5.73	4.85	8.81	7.92	35.3	81.2
18/09/91	20:49	1.94	2.00	1.08	4.09	2.82	55.4	85.1
19/09/91	22:09	16.08	3.39	2.15	6.19	6.57	49.8	68.9
25/09/91	21:43	12.12	10.17	9.30	12.88	12.42	18.8	72.0
26/09/91	21:23	7.26	6.10	6.02	8.01	5.95	16.8	75.9
29/09/91	22:01	27.44	10.29	8.85	15.36	14.75	41.8	67.4
01/10/91	21:18	12.38	10.69	9.91	13.66	11.69	23.2	75.2
02/10/91	20:58	12.95	11.59	11.09	14.49	14.11	48.3	79.2
03/10/91	20:37	10.18	10.59	10.41	13.81	9.81	63.1	83.1
03/10/91	22:18	19.65	15.63	14.58	19.17	18.66	57.0	62.9
07/10/91	20:54	9.01	7.75	6.84	12.06	8.91	51.9	78.6
08/10/91	22:14	16.94	10.67	9.17	15.52	15.37	53.9	62.2
09/10/91	21:52	15.36	12.12	11.40	14.62	13.66	31.6	66.1
10/10/91	21:31	13.75	9.90	9.03	12.21	10.30	2.3	70.1
13/10/91	22:10	19.60	16.37	15.52	17.39	19.35	50.3	61.6
14/10/91	21:48	22.48	21.03	20.26	21.84	24.01	25.6	65.6
15/10/91	21:27	13.30	11.52	10.73	14.35	12.06	9.5	69.6
17/10/91	20:46	8.31	5.47	5.34	9.20	5.41	57.9	77.6
18/10/91	22:05	22.18	18.51	17.58	19.27	21.88	46.3	61.2
23/10/91	22:01	20.99	17.43	16.40	19.25	18.44	41.6	60.9
30/10/91	21:14	15.00	11.97	11.26	15.42	11.93	29.3	68.8
31/10/91	20:53	11.78	8.85	8.29	13.30	10.26	51.7	72.9
02/04/92	21:58	20.45	18.71	17.58	21.78	21.81	37.5	73.4
20/04/92	22:17	13.87	7.53	7.07	11.26	10.52	55.8	73.1
29/05/92	21:48	0.12	0.18	0.72	1.86	1.56	25.6	84.6

Table 13: Daytime NOAA-11 AVHRR brightness temperatures ($^{\circ}\text{C}$) and in situ validation temperatures ($^{\circ}\text{C}$) for the pasture land at the Uardry field site. The date, time (hours:minutes), satellite surface zenith angle (ϕ in degrees) and solar zenith angle (ψ in degrees) are given for the pixel closest to the field site.

D/M/Y	Time (UT)	T_3	T_4	T_5	T_v	T_a	T_g	ϕ	ψ
10/07/92	05:38	13.97	11.00	10.90	13.20	13.30	16.60	16.7	73.0
16/07/92	06:08	14.26	12.06	12.17	13.50	15.80	17.90	47.5	77.0
27/07/92	05:36	17.56	14.34	14.09	15.70	16.20	19.30	23.8	70.3
29/07/92	05:12	20.83	16.52	15.31	20.80	17.90	21.60	51.8	66.4
30/07/92	04:59	20.52	17.82	16.94	22.30	18.10	22.70	60.8	64.4
31/07/92	06:28	12.06	9.56	9.47	12.90	12.80	13.90	49.3	78.1
02/08/92	06:04	15.30	12.60	12.48	15.40	13.10	16.70	20.8	73.7
09/08/92	06:21	12.19	9.77	9.59	12.70	12.70	14.60	40.9	75.4
11/08/92	05:55	16.74	13.95	13.84	16.70	15.60	17.80	7.3	70.6
21/08/92	05:37	22.74	14.90	13.88	19.80	15.10	20.40	25.9	65.7
24/08/92	06:41	19.21	14.00	13.50	19.00	14.20	19.50	67.1	76.5
28/08/92	05:53	20.88	17.62	17.36	20.60	16.50	21.20	1.0	67.1
08/09/92	05:22	20.21	15.85	15.21	20.80	14.90	21.40	46.4	59.4
09/09/92	05:09	22.49	17.47	16.15	24.10	16.70	25.90	56.5	57.1
17/09/92	05:14	22.86	18.65	17.31	24.90	17.50	24.90	53.9	56.1
22/09/92	05:54	24.06	20.51	19.09	24.40	21.90	26.20	3.9	62.5
12/10/92	05:15	22.55	19.91	18.80	26.80	20.30	27.50	55.1	51.3
13/10/92	05:03	24.17	20.97	19.44	29.80	24.60	30.70	63.2	48.9
13/12/92	06:13	30.65	24.87	22.75	30.60	28.10	34.40	10.7	53.1
14/12/92	06:00	34.92	29.45	28.08	31.90	28.10	36.50	9.8	50.3
21/12/92	06:17	36.60	28.79	25.79	34.50	32.90	38.60	15.7	53.0
29/12/92	06:20	35.86	30.55	28.94	32.40	28.00	38.40	5.0	52.9
31/12/92	05:56	43.40	37.65	34.81	41.20	37.00	50.10	20.0	47.8

Table 14: Nighttime NOAA-11 AVHRR brightness temperatures ($^{\circ}\text{C}$) and in situ validation temperatures ($^{\circ}\text{C}$) for the pasture land at the Uardry field site. The date, time (hours:minutes) and satellite surface zenith angle (ϕ in degrees) are given for the pixel closest to the field site.

D/M/Y	Time (UT)	T_3	T_4	T_5	T_v	T_a	T_g	ϕ
09/07/92	17:15	-0.64	-0.56	-0.06	1.9	1.8	1.4	23.3
13/07/92	16:26	-3.15	-2.47	-1.73	1.0	0.9	0.1	46.2
15/07/92	16:03	-1.36	-0.20	0.70	1.5	1.6	1.2	63.4
15/07/92	17:43	-2.75	-2.95	-1.89	0.7	0.1	0.1	54.5
16/07/92	17:31	-0.19	0.69	1.36	1.9	2.6	1.5	43.4
26/07/92	17:11	-3.55	-3.66	-3.05	-0.4	-1.7	-1.2	16.0
03/08/92	17:16	-1.94	-1.90	-1.24	-0.1	-3.0	-1.2	11.6
06/08/92	16:39	0.73	0.94	1.26	3.3	2.3	1.7	24.6
12/08/92	17:08	2.66	2.74	3.03	4.4	5.7	4.0	8.0
17/08/92	16:08	-1.56	-0.37	-0.05	2.4	1.8	1.6	62.4
17/08/92	17:49	-2.59	-1.55	-1.26	1.8	1.2	0.6	56.4
24/08/92	16:24	-3.05	-2.37	-1.47	0.1	-0.4	-0.6	51.8
27/08/92	17:29	3.87	4.51	4.92	6.5	7.5	6.5	36.3
02/09/92	16:17	2.27	2.67	3.36	5.5	5.2	4.1	60.8
03/09/92	17:45	-1.05	-0.34	0.08	3.7	2.2	1.8	52.2
06/09/92	17:09	3.38	4.11	4.36	6.8	6.2	6.2	5.3
07/09/92	16:57	1.42	1.45	1.91	4.5	2.7	3.1	14.6
08/09/92	16:45	-1.16	-1.14	-0.66	2.9	1.2	1.1	31.9
13/09/92	17:25	-3.05	-2.88	-2.09	1.9	0.9	-2.0	29.3
15/09/92	17:02	1.73	1.92	2.23	4.5	3.5	2.3	8.9
16/09/92	16:49	2.29	2.73	3.07	4.7	3.9	3.2	27.2
20/09/92	17:42	-1.30	-0.76	-0.05	3.2	0.8	2.4	50.9
22/09/92	17:18	4.37	5.29	5.85	7.8	5.9	7.5	16.4
30/09/92	17:22	3.94	3.80	4.57	7.6	5.6	5.1	21.5
06/10/92	16:11	6.74	6.32	6.50	10.3	7.0	8.2	63.5
06/10/92	17:51	5.11	5.78	6.11	9.9	6.4	7.5	53.1
11/10/92	16:51	3.27	3.69	4.29	9.3	4.7	6.0	29.1
12/10/92	16:39	6.28	7.74	8.32	11.7	8.6	9.3	43.3
13/10/92	16:27	7.80	9.04	9.18	13.6	11.6	12.2	53.9
08/12/92	16:55	11.99	12.90	12.72	18.2	18.6	14.2	32.3
09/12/92	16:44	11.95	12.78	12.88	17.8	14.1	15.4	46.0
26/12/92	16:40	11.40	12.24	12.10	15.4	12.2	13.6	51.5
29/12/92	17:44	11.89	13.00	13.36	16.1	13.1	14.9	37.5
31/12/92	17:20	18.43	19.10	18.73	21.8	20.4	22.4	0.4

Table 15: Morning NOAA-12 AVHRR brightness temperatures ($^{\circ}\text{C}$) and in situ validation temperatures ($^{\circ}\text{C}$) for the pasture land at the Uardry field site. The date, time (hours:minutes), satellite surface zenith angle (ϕ in degrees) and the solar zenith angle (ψ in degrees) are given for the pixel closest to the field site.

D/M/Y	Time (UT)	T_3	T_4	T_5	T_v	T_a	T_g	ϕ
09/07/92	17:15	-0.64	-0.56	-0.06	1.9	1.8	1.4	23.3
13/07/92	16:26	-3.15	-2.47	-1.73	1.0	0.9	0.1	46.2
15/07/92	16:03	-1.36	-0.20	0.70	1.5	1.6	1.2	63.4
15/07/92	17:43	-2.75	-2.95	-1.89	0.7	0.1	0.1	54.5
16/07/92	17:31	-0.19	0.69	1.36	1.9	2.6	1.5	43.4
26/07/92	17:11	-3.55	-3.66	-3.05	-0.4	-1.7	-1.2	16.0
03/08/92	17:16	-1.94	-1.90	-1.24	-0.1	-3.0	-1.2	11.6
06/08/92	16:39	0.73	0.94	1.26	3.3	2.3	1.7	24.6
12/08/92	17:08	2.66	2.74	3.03	4.4	5.7	4.0	8.0
17/08/92	16:08	-1.56	-0.37	-0.05	2.4	1.8	1.6	62.4
17/08/92	17:49	-2.59	-1.55	-1.26	1.8	1.2	0.6	56.4
24/08/92	16:24	-3.05	-2.37	-1.47	0.1	-0.4	-0.6	51.8
27/08/92	17:29	3.87	4.51	4.92	6.5	7.5	6.5	36.3
02/09/92	16:17	2.27	2.67	3.36	5.5	5.2	4.1	60.8
03/09/92	17:45	-1.05	-0.34	0.08	3.7	2.2	1.8	52.2
06/09/92	17:09	3.38	4.11	4.36	6.8	6.2	6.2	5.3
07/09/92	16:57	1.42	1.45	1.91	4.5	2.7	3.1	14.6
08/09/92	16:45	-1.16	-1.14	-0.66	2.9	1.2	1.1	31.9
13/09/92	17:25	-3.05	-2.88	-2.09	1.9	0.9	-2.0	29.3
15/09/92	17:02	1.73	1.92	2.23	4.5	3.5	2.3	8.9
16/09/92	16:49	2.29	2.73	3.07	4.7	3.9	3.2	27.2
20/09/92	17:42	-1.30	-0.76	-0.05	3.2	0.8	2.4	50.9
22/09/92	17:18	4.37	5.29	5.85	7.8	5.9	7.5	16.4
30/09/92	17:22	3.94	3.80	4.57	7.6	5.6	5.1	21.5
06/10/92	16:11	6.74	6.32	6.50	10.3	7.0	8.2	63.5
06/10/92	17:51	5.11	5.78	6.11	9.9	6.4	7.5	53.1
11/10/92	16:51	3.27	3.69	4.29	9.3	4.7	6.0	29.1
12/10/92	16:39	6.28	7.74	8.32	11.7	8.6	9.3	43.3
13/10/92	16:27	7.80	9.04	9.18	13.6	11.6	12.2	53.9
08/12/92	16:55	11.99	12.90	12.72	18.2	18.6	14.2	32.3
09/12/92	16:44	11.95	12.78	12.88	17.8	14.1	15.4	46.0
26/12/92	16:40	11.40	12.24	12.10	15.4	12.2	13.6	51.5
29/12/92	17:44	11.89	13.00	13.36	16.1	13.1	14.9	37.5
31/12/92	17:20	18.43	19.10	18.73	21.8	20.4	22.4	0.4

Table 16: Evening NOAA-12 AVHRR brightness temperatures ($^{\circ}\text{C}$) and in situ validation temperatures ($^{\circ}\text{C}$) for the pasture land at the Uardry field site. The date, time (hours:minutes) and satellite surface zenith angle (ϕ in degrees) are given for the pixel closest to the field site.

D/M/Y	Time (UT)	T_3	T_4	T_5	T_v	T_a	T_g	ϕ
09/07/92	10:57	0.89	1.45	1.75	4.9	5.1	4.4	58.2
12/07/92	09:57	0.76	2.21	2.49	5.2	6.3	6.0	26.2
29/07/92	10:32	4.73	5.88	6.13	7.1	8.4	7.8	34.4
02/08/92	10:46	-2.31	-2.25	-1.74	1.6	2.3	2.3	50.2
03/08/92	10:26	-2.06	-1.58	-1.26	1.5	0.9	1.0	25.8
06/08/92	09:21	3.73	4.74	4.57	8.1	7.9	7.7	59.7
09/08/92	09:58	0.74	1.36	1.49	4.2	3.7	3.9	19.8
11/08/92	09:14	2.09	3.59	3.78	6.7	6.9	6.9	64.0
17/08/92	10:27	1.89	3.07	3.03	6.0	6.1	6.3	28.8
18/08/92	10:06	-0.12	-0.03	0.55	3.1	2.8	2.3	5.8
24/08/92	09:38	-0.99	-0.53	-0.18	2.9	1.8	3.5	45.6
30/08/92	09:10	3.94	3.91	2.81	7.9	8.6	7.7	66.8
02/09/92	09:47	4.70	4.98	4.99	8.6	7.3	9.2	35.9
03/09/92	09:25	1.81	2.86	2.85	7.2	6.2	7.5	57.3
06/09/92	10:02	3.25	4.63	4.65	8.6	7.9	9.2	13.7
10/09/92	10:16	3.91	5.04	4.88	9.0	7.5	10.4	11.8
29/09/92	10:12	2.23	3.29	3.14	8.5	4.8	8.2	4.1
30/09/92	09:54	4.27	5.91	6.00	11.0	8.5	9.9	30.7
05/10/92	09:44	6.89	7.64	7.49	12.7	8.8	10.3	39.2
12/10/92	10:35	7.92	9.33	9.46	14.6	10.5	13.9	39.8
13/10/92	10:14	10.96	11.62	11.39	16.5	13.7	16.3	8.8
08/12/92	10:19	15.44	15.93	15.02	21.1	19.6	22.0	18.2
09/12/92	09:58	18.96	18.66	17.87	21.4	19.3	22.9	18.4
10/12/92	09:36	17.62	18.08	17.29	23.7	22.2	25.1	46.5

Table 17: ATSR brightness temperatures, in situ temperatures (T_s), and viewing angles for validation data from the Walpeup site. The in situ values have been interpolated to the ATSR overpass time. In all cases the in situ data were obtained within one hour of the ATSR data. T_{11}^n and T_{11}^f are the 11 μm ATSR nadir and forward brightness temperatures; T_{12}^n and T_{12}^f are the 12 μm ATSR nadir and forward brightness temperatures. All temperatures are in $^{\circ}\text{C}$. ϕ_n , ϕ_f , and ψ are the nadir and forward surface zenith angles, and solar zenith angles respectively.

Date	Time (UT)	T_{11}^n	T_{11}^f	T_{12}^n	T_{12}^f	T_s	ϕ_n	ϕ_f	ψ
03/09/91	13:27	5.03	4.33	4.99	4.76	7.63	2.5	54.9	—
06/09/91	13:27	10.26	10.41	10.59	10.38	11.90	2.5	54.9	—
06/10/91	13:27	8.52	6.68	8.50	5.43	13.85	2.5	54.9	—
09/10/91	13:27	8.06	6.52	8.06	6.39	11.37	2.5	54.9	—
12/10/91	13:27	12.45	11.51	12.62	11.46	16.99	2.5	54.9	—
21/10/91	13:27	10.26	9.19	10.06	9.16	14.82	2.5	54.9	—
05/10/91	00:35	29.19	26.86	27.49	25.41	31.88	5.6	54.8	34.2

Table 18: ATSR brightness temperatures T_{11}^n , T_{11}^f , T_{12}^n , and T_{12}^f , in situ temperatures (T_g), and viewing angles (degrees) for the validation data obtained from the Uardry site. All temperatures are in °C. ϕ_n , ϕ_f and ψ are the nadir and forward surface zenith angles, and solar zenith angles respectively.

Date	Time (UT)	T_{11}^n	T_{11}^f	T_{12}^n	T_{12}^f	T_g	ϕ_n	ϕ_f	ψ
03/08/92	13:03	-2.01	-2.28	-1.21	-1.67	0.02	2.8	54.9	—
07/08/92	00:21	13.33	12.93	12.91	12.43	14.98	14.6	53.6	58.9
28/08/92	13:17	0.54	-0.78	1.00	-0.08	2.84	13.9	53.7	—
10/09/92	13:09	4.07	3.31	4.81	3.28	6.76	14.2	53.7	—
13/09/92	13:15	0.03	-1.80	0.32	-1.18	3.68	19.5	52.6	—
14/09/92	00:27	21.23	20.71	20.80	20.00	22.40	19.2	52.7	45.8
17/09/92	00:33	20.54	19.16	19.18	17.61	23.56	7.8	54.6	43.9
29/09/92	13:12	3.55	2.50	3.86	2.90	5.54	19.8	52.6	--
05/10/92	13:23	6.26	4.08	6.24	4.53	9.82	2.5	55.0	—
12/10/92	13:03	8.47	8.09	8.82	8.24	12.02	2.9	54.9	—
21/10/92	13:20	7.39	7.07	7.67	7.30	10.00	8.3	54.5	—
22/10/92	00:32	27.39	22.53	26.41	21.24	34.88	8.0	54.5	31.5
09/12/92	00:24	32.69	27.71	30.19	24.85	42.17	20.0	52.5	26.0
10/01/93	00:18	34.96	29.45	33.10	27.67	42.50	9.0	54.4	30.4
13/01/93	00:24	37.66	34.79	36.09	33.29	45.60	20.3	52.5	29.6
19/01/93	00:35	35.21	30.33	32.88	27.47	44.03	2.1	55.0	28.5
01/02/93	00:27	38.84	33.22	36.85	30.47	51.16	19.2	52.7	32.5
30/03/93	00:35	23.48	21.57	22.21	19.93	29.62	2.3	55.0	45.5
30/12/92	13:10	18.31	17.09	18.07	17.09	23.53	8.3	54.5	—
12/01/93	13:10	13.13	11.91	13.34	12.55	18.98	19.9	52.5	—
18/01/93	13:21	18.75	17.13	18.16	16.28	22.88	2.6	54.9	—
28/01/93	13:07	17.90	15.66	17.36	15.51	22.73	14.2	53.7	—
31/01/93	13:12	23.09	21.73	22.52	20.34	27.90	19.6	52.6	—
03/02/93	13:18	23.17	21.24	23.64	21.17	28.85	8.3	54.5	—
13/02/93	13:04	21.21	20.24	20.76	19.63	24.17	8.5	54.5	—
04/03/93	13:07	11.19	10.36	11.47	10.38	16.33	14.2	53.7	—
07/03/93	13:12	13.95	13.09	14.15	12.77	18.58	19.6	52.6	—
20/03/93	13:04	15.41	15.67	14.41	15.05	19.10	8.5	54.5	—
26/03/93	13:15	14.30	13.65	14.14	13.39	16.52	13.9	53.7	—
29/03/93	13:21	9.54	8.83	9.36	8.89	11.95	2.5	55.0	—

Table 19: Mean monthly climatological atmospheric parameters for the Walpeup site. See text for definitions of the parameters. The units for all radiances are $\text{mW}/(\text{m}^2\text{cm}^{-1}\text{sr})$. T_0 is the monthly mean temperature at 1000 mb.

Month	T_0 K	τ_4	τ_5	γ_{45}	$R_4\downarrow$	$R_5\downarrow$	$R_4\uparrow$	$R_5\uparrow$	PW g cm^{-2}
Jan	295.60	0.811	0.747	2.997	16.51	26.04	15.53	25.68	1.46
Feb	295.50	0.811	0.747	2.987	16.80	26.20	15.60	26.06	1.42
Mar	293.20	0.824	0.765	3.023	15.03	23.58	13.97	23.25	1.31
Apr	289.85	0.838	0.785	3.068	13.02	20.44	12.03	20.23	1.18
May	285.70	0.858	0.814	3.214	10.83	17.02	9.88	16.62	0.98
Jun	282.60	0.868	0.829	3.329	9.61	15.01	8.70	14.66	0.90
Jul	282.30	0.875	0.838	3.450	8.99	13.96	8.07	13.62	0.84
Aug	283.65	0.875	0.838	3.445	9.01	14.03	8.10	13.64	0.84
Sep	286.60	0.872	0.835	3.428	9.52	14.84	8.57	14.47	0.87
Oct	289.95	0.862	0.819	3.294	10.86	16.86	9.82	16.44	1.00
Nov	292.05	0.855	0.811	3.246	11.64	18.05	10.56	17.65	1.07
Dec	294.10	0.843	0.792	3.136	13.09	20.35	12.13	20.22	1.19

Table 20: Mean monthly climatological atmospheric parameters for the Hay site. The units for all radiances are $\text{mW}/(\text{m}^2\text{cm}^{-1}\text{sr})$. T_0 is the monthly mean temperature at 1000 mb.

Month	T_0 K	τ_4	τ_5	τ_{45}	$R_4\downarrow$	$R_5\downarrow$	$R_4\uparrow$	$R_5\uparrow$	PW g cm^{-2}
Jan	295.08	0.809	0.745	2.974	16.58	26.11	15.59	25.75	1.46
Feb	294.78	0.804	0.737	2.954	17.23	26.99	16.13	26.80	1.46
Mar	292.45	0.819	0.758	2.988	15.27	24.01	14.24	23.75	1.35
Apr	288.83	0.837	0.784	3.056	12.97	20.42	11.99	20.11	1.18
May	284.60	0.856	0.811	3.183	10.80	16.99	9.86	16.60	1.01
Jun	281.70	0.868	0.829	3.318	9.48	14.82	8.57	14.46	0.91
Jul	281.25	0.875	0.838	3.425	8.85	13.77	7.95	13.41	0.84
Aug	282.65	0.874	0.836	3.398	8.98	14.02	8.09	13.64	0.86
Sep	285.45	0.869	0.830	3.360	9.62	15.02	8.69	14.65	0.90
Oct	288.88	0.856	0.812	3.223	11.13	17.34	10.12	17.00	1.04
Nov	291.05	0.851	0.804	3.184	11.90	18.53	10.85	18.21	1.11
Dec	293.48	0.838	0.786	3.096	13.37	20.85	12.36	20.66	1.22

Table 21: Emissivity measurements and error estimates for the soils at Walpeup and Hay, and for the growing and senesced wheat crops at Walpeup.

Surface type	Emissivity		Emissivity error	
	11 μm	12 μm	11 μm	12 μm
Walpeup-sandy soil	0.955	0.965	± 0.005	± 0.005
Walpeup-growing wheat†	0.976		± 0.015	
Walpeup-senesced wheat†	0.980		± 0.007	
Hay soil (red clay)	0.958	0.967	± 0.005	± 0.005
Hay soil/vegetation mixture	0.978	0.982	± 0.005	± 0.005

†Broadband (10-12.5 μm) measurements.

CSIRO DIVISION OF ATMOSPHERIC RESEARCH TECHNICAL PAPERS

- No. 1 Galbally, I. E.; Roy, C. R.; O'Brien, R. S.; Ridley, B. A.; Hastie, D. R.; Evans, W. J. F.; McElroy, C. T.; Kerr, J. B.; Hyson, P.; Knight, W.; Laby, J. E.
Measurements of trace composition of the Austral stratosphere: chemical and meteorological data. 1983. 31 p.
- No. 2 Enting, I. G.
Error analysis for parameter estimates from constrained inversion. 1983. 18 p.
- No. 3 Enting, I. G.; Pearman, G. I.
Refinements to a one-dimensional carbon cycle model. 1983. 35 p.
- No. 4 Francey, R. J.; Barbetti, M.; Bird, T.; Beardsmore, D.; Coupland, W.; Dolezal, J. E.; Farquhar, G. D.; Flynn, R. G.; Fraser, P. J.; Gifford, R. M.; Goodman, H. S.; Kunda, B.; McPhail, S.; Nanson, G.; Pearman, G. I.; Richards, N. G.; Sharkey, T. D.; Temple, R. B.; Weir, B.
Isotopes in tree rings. 1984. 86 p.
- No. 5 Enting, I. G.
Techniques for determining surface sources from surface observations of atmospheric constituents. 1984. 30 p.
- No. 6 Beardsmore, D. J.; Pearman, G. I.; O'Brien, R. C.
The CSIRO (Australia) Atmospheric Carbon Dioxide Monitoring Program: surface data. 1984. 115 p.
- No. 7 Scott, John C.
High speed magnetic tape interface for a microcomputer. 1984. 17 p.
- No. 8 Galbally, I. E.; Roy, C. R.; Elsworth, C. M.; Rabich, H. A. H.
The measurement of nitrogen oxide (NO, NO₂) exchange over plant/soil surfaces. 1985. 23 p.
- No. 9 Enting, I. G.
A strategy for calibrating atmospheric transport models. 1985. 25 p.
- No. 10 O'Brien, D. M.
TOVPIX: software for extraction and calibration of TOVS data from the high resolution picture transmission from TIROS-N satellites. 1985. 41 p.
- No. 11 Enting, I. G.; Mansbridge, J. V.
Description of a two-dimensional atmospheric transport model. 1986. 22 p.
- No. 12 Everett, J. R.; O'Brien, D. M.; Davis, T. J.
A report on experiments to measure average fibre diameters by optical fourier analysis. 1986. 22 p.

- No. 13 Enting, I. G.
A signal processing approach to analysing background atmospheric constituent data. 1986. 21 p.
- No. 14 Enting, I. G.; Mansbridge, J. V.
Preliminary studies with a two-dimensional model using transport fields derived from a GCM. 1987. 47 p.
- No. 15 O'Brien, D. M.; Mitchell, R. M.
Technical assessment of the joint CSIRO/Bureau of Meteorology proposal for a geostationary imager/ sounder over the Australian region. 1987. 53 p.
- No. 16 Galbally, I. E.; Manins, P. C.; Ripari, L.; Bateup, R.
A numerical model of the late (ascending) stage of a nuclear fireball. 1987. 89 p.
- No. 17 Durre, A. M.; Beer, T.
Wind information prediction study: Annaburroo meteorological data analysis. 1989. 30 p. + diskette.
- No. 18 Mansbridge, J. V.; Enting, I. G.
Sensitivity studies in a two-dimensional atmospheric transport model. 1989. 33 p.
- No. 19 O'Brien, D. M.; Mitchell, R. M.
Zones of feasibility for retrieval of surface pressure from observations of absorption in the A band of oxygen. 1989. 12 p.
- No. 20 Evans, J. L.
Envisaged impacts of enhanced greenhouse warming on tropical cyclones in the Australian region. 1990. 31 p. [Out of print]
- No. 21 Whetton, P. H.; Pittock, A. B.
Australian region intercomparison of the results of some general circulation models used in enhanced greenhouse experiments. 1991. 73 p. [Out of print]
- No. 22 Enting, I. G.
Calculating future atmospheric CO₂ concentrations. 1991. 32 p.
- No. 23 Kowalczyk, E. A.; Garratt, J. R.; Krummel, P. B.
A soil-canopy scheme for use in a numerical model of the atmosphere — 1D stand-alone model. 1992. 56 p.
- No. 24 Physick, W. L.; Noonan, J.A.; McGregor, J.L.; Hurley, P.J.; Abbs, D.J.; Manins, P.C.
LADM: A Lagrangian Atmospheric Dispersion Model. 1994. 137 p.
- No. 25 Enting, I. G.
Constraining the atmospheric carbon budget: a preliminary assessment. 1992. 28 p.
- No. 26 McGregor, J. L.; Gordon, H. B.; Watterson, I. G.; Dix, M. R.; Rotstayn, L. D.
The CSIRO 9-level atmospheric general circulation model. 1993. 89 p.

- No. 27 Enting, I. G.; Lassey, K. R.
The CSIRO 9-level atmospheric general circulation model. with appendix by R. A. Houghton. 1993. 42 p.
- No. 28 [Not published]
- No. 29 Enting, I. G.; Trudinger, C. M.; Francey, R. J.; Granek, H.
Synthesis inversion of atmospheric CO₂ using the GISS tracer transport model. 1993. 44 p.
- No. 30 O'Brien, D. M.
Radiation fluxes and cloud amounts predicted by the CSIRO nine level GCM and observed by ERBE and ISCCP. 1993. 37 p.
- No. 32 Kowalczyk, E.A.; Garratt, J.R.; Krummel, P.B.
Implementation of a soil-canopy scheme into the CSIRO GCM — regional aspects of the model response